

We are IntechOpen, the world's leading publisher of Open Access books Built by scientists, for scientists

4,800

Open access books available

122,000

International authors and editors

135M

Downloads

Our authors are among the

154

Countries delivered to

TOP 1%

most cited scientists

12.2%

Contributors from top 500 universities



WEB OF SCIENCE™

Selection of our books indexed in the Book Citation Index
in Web of Science™ Core Collection (BKCI)

Interested in publishing with us?
Contact book.department@intechopen.com

Numbers displayed above are based on latest data collected.
For more information visit www.intechopen.com



OFDM Communications with Cooperative Relays

H. Lu¹, H. Nikookar¹ and T. Xu²

¹*International Research Centre for Telecommunications and Radar (IRCTR)*

²*Circuits and Systems Group (CAS)*

Dept. EEMCS, Delft University of Technology

Mekelweg 4, 2628 CD, Delft,

The Netherlands

1. Introduction

1.1 Cooperative relay communications

Signal fading due to multi-path propagation is one of the major impairments to meet the demands of next generation wireless networks for high data rate services. To mitigate the fading effects, time, frequency, and spatial diversity techniques or their hybrid can be used. Among different types of diversity techniques, spatial diversity is of special interest as it does not incur system losses in terms of delay and bandwidth efficiency.

Recently, cooperative diversity in wireless network has received great interest and is regarded as a promising technique to mitigate multi-path fading, which results in a fluctuation in the amplitude of the received signal. Cooperative communications is a new communication paradigm which generates independent paths between the user and the base station by introducing a relay channel. The relay channel can be thought of as an auxiliary channel to the direct channel between the source and destination. The basic idea behind cooperation is that several users in a network pool their resources in order to form a virtual antenna array which creates spatial diversity (Laneman et al., 2004; Sendonaris et al., Part I, 2003; Sendonaris et al., Part II, 2003). Since the relay node is usually several wavelengths distant from the source, the relay channel is guaranteed to fade independently from the direct channel, which introduces a full-rank Multiple-input-multiple-output (MIMO) channel between the source and the destination. This cooperative spatial diversity leads to an increased exponential decay rate in the error probability with increasing signal-to-noise ratio (SNR) (Liu et al., 2009).

Before discussing cooperative OFDM, let us first review some fundamental knowledge of OFDM and MIMO, which is associated with the cooperative OFDM study in this chapter.

1.2 Physical layer of cooperative wireless networks (OFDM & MIMO)

1.2.1 OFDM basics

In the modern wireless communication, OFDM technology has been widely used due to its spectral efficiency and inherent flexibility in allocating power and bit rate over distinct subcarriers which are orthogonal to each other. Different from a serial transmission, OFDM

Source: Communications and Networking, Book edited by: Jun Peng,
ISBN 978-953-307-114-5, pp. 434, September 2010, Sciyo, Croatia, downloaded from SCIYO.COM

is a multi-carrier block transmission, where, as the name suggests, information-bearing symbols are processed in blocks at both the transmitter and the receiver.

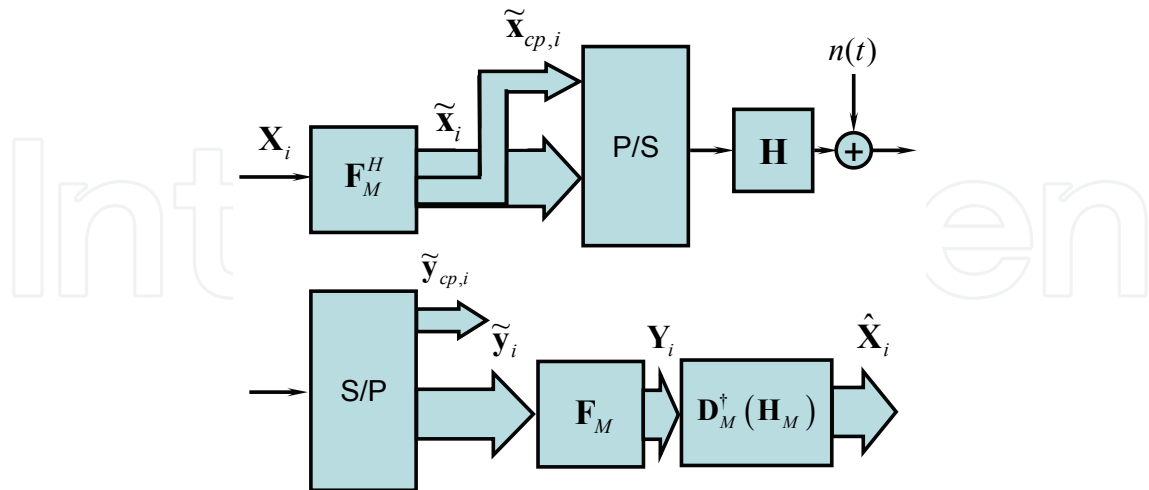


Fig. 1. Discrete-time block equivalent models of CP-OFDM, top: transmitter & channel, bottom: receiver.

A number of benefits the OFDM brings to cooperative relay systems originate from the basic features that OFDM possesses. To appreciate those, we first outline Cyclic Prefix (CP)-OFDM's operation using the discrete-time baseband equivalent block model of a single-transceiver system depicted in Fig.1, where \mathbf{X}_i is the so-called frequency signal at the i -th time symbol duration in one OFDM frame, then it will be transferred as $\tilde{\mathbf{x}}_i$ in the time domain by the M -point inverse fast Fourier transform (IFFT) matrix $\mathbf{F}_M^{-1} = \mathbf{F}_M^H$ with (m, k) -th entry $\exp(j2\pi mk / M) / \sqrt{M}$, i.e., $\tilde{\mathbf{x}}_i = \mathbf{F}_M^H \mathbf{X}_i$, \mathbf{F}_M is the M -point fast Fourier transform (FFT) matrix. where $(\cdot)^H$ denotes conjugate transposition, $(\cdot)^\dagger$ denotes matrix pseudoinverse, and $(\cdot)^{-1}$ denotes matrix inversion and m, k denote the index in frequency and time domain, respectively. Applying the triangle inequality to the M -point IFFT definition shows that the entries of $\mathbf{F}_M^H \mathbf{X}_i$ have magnitudes that can exceed those of \mathbf{X}_i by a factor as high as M . In other words, IFFT processing can increase the peak to average power ratio (PAPR) by a factor as high as the number of subcarriers (which in certain applications can exceed 1000). Then a CP of length D is inserted between each $\tilde{\mathbf{x}}_i$ to form the redundant OFDM symbols $\tilde{\mathbf{x}}_{cp,i}$, which are sequentially transmitted through the channel. The total number of the time domain signals in each OFDM symbol is, thus, $C = M + D$. If we define $\mathbf{F}_{cp} := [\mathbf{F}_D, \mathbf{F}_M]^H$ as the $C \times M$ expanded IFFT matrix, where \mathbf{F}_D is the last D columns of \mathbf{F}_M , that way, the redundant OFDM symbol to be transmitted can also be expressed as $\tilde{\mathbf{x}}_{cp,i} = \mathbf{F}_{cp} \mathbf{X}_i$. With $(\cdot)^T$ denotes transposition, and assuming no channel state information (CSI) to be available at the transmitter, then the received symbol $\tilde{\mathbf{y}}_{cp,i}$ at the i -th time symbol duration can be written as:

$$\tilde{\mathbf{y}}_{cp,i} = \mathbf{H} \mathbf{F}_{cp} \mathbf{X}_i + \mathbf{H}_{ISI} \mathbf{F}_{cp} \mathbf{X}_{i-1} + \tilde{\mathbf{n}}_{C,i} \quad (1)$$

where \mathbf{H} is the $C \times C$ lower triangular Toeplitz filtering matrix with first column $[h_1 \cdots h_L \ 0 \cdots 0]^T$, where L is the channel order (i.e., $h_i = 0, \forall i > L$), \mathbf{H}_{ISI} is the $C \times C$ upper triangular Toeplitz filtering matrix with first row $[0 \cdots 0 \ h_L \cdots h_2]$, which captures inter-

symbol interference (ISI), $\tilde{\mathbf{n}}_{C,i}$ denotes the additive white Gaussian noise (AWGN) vector with variance N_0 and Length C . After removing the CP at the receiver, ISI is also discarded, and (1) can be rewritten as:

$$\tilde{\mathbf{y}}_i = \mathbf{C}_M(\mathbf{h})\mathbf{F}_M^H\mathbf{X}_i + \tilde{\mathbf{n}}_{M,i} \quad (2)$$

where $\mathbf{C}_M(\mathbf{h})$ is $M \times M$ circulant matrix with first row $[h_1 \ 0 \cdots 0 \ h_L \cdots h_2]$, and $\tilde{\mathbf{n}}_{M,i}$ is a vector formed by the last M elements of $\tilde{\mathbf{n}}_{C,i}$.

The procedure of adding and removing CP forces the linear convolution with the channel impulse response to resemble a circular convolution. Equalization of CP-OFDM transmissions ties to the well known property that a circular convolution in the time domain, is equivalent to a multiplication operation in the frequency domain. Hence, the circulant matrix can be diagonalized by post- (pre-) multiplication by (I)FFT matrices, and only a single-tap frequency domain equalizer is sufficient to resolve the multipath effect on the transmitted signal. After demodulation with the FFT matrix, the received signal is given by:

$$\begin{aligned} \mathbf{Y}_i &= \mathbf{F}_M \mathbf{C}_M(\mathbf{h}) \mathbf{F}_M^H \mathbf{X}_i + \mathbf{F}_M \tilde{\mathbf{n}}_{M,i} \\ &= \text{diag}(H_1 \cdots H_M) \mathbf{X}_i + \mathbf{F}_M \tilde{\mathbf{n}}_{M,i} \\ &= \mathbf{D}_M(\mathbf{H}_M) \mathbf{X}_i + \mathbf{n}_{M,i} \end{aligned} \quad (3)$$

where $\mathbf{H}_M = [H_1 \cdots H_M]^T = \sqrt{M} \mathbf{F}_M \mathbf{h}$, with

$$H_k \equiv H(2\pi k / M) := \sum_{l=1}^L h_l e^{-j2\pi kl / M} \quad (4)$$

denoting the channel's transfer function on the k -th subcarrier, $\mathbf{D}_M(\mathbf{H}_M)$ stands for the $M \times M$ diagonal matrix with \mathbf{H}_M on its diagonal, $\mathbf{n}_{M,i} := \mathbf{F}_M \tilde{\mathbf{n}}_{M,i}$.

Equations (3) and (4) show that an OFDM system which relies on M subcarriers to transmit the symbols of each block \mathbf{X}_i , converts an FIR frequency-selective channel to an equivalent set of M flat fading subchannels. This is intuitively reasonable since each narrowband subcarrier that is used to convey each information-bearing symbol per OFDM block "sees" a narrow portion of the broadband frequency-selective channel which can be considered frequency flat. This scalar model enables simple equalization of the FIR channel (by dividing (3) with the corresponding scalar subchannel \mathbf{H}_M) as well as low-complexity decoding across subchannels using (Muquet et al., 2009; Wang & Giannakis, 2000). Transmission of symbols over subcarriers also allows for a flexible allocation of the available bandwidth to multiple users operating with possibly different rate requirements imposed by multimedia applications, which may include communication of data, audio, or video. When CSI is available at the transmitter side, power and bits can be adaptively loaded per OFDM subcarrier, depending on the strength of the intended subchannel. Because of orthogonality of OFDM subcarriers, OFDM system exhibits robustness to the narrow band interference.

The price paid for OFDM's attractive features in equalization, decoding, and possibly adaptive power and bandwidth allocation is its sensitivity to subcarrier drifts and the high PAPR that IFFT processing introduces to the entries of each block transmitted. Subcarrier

drifts come either from the carrier-frequency and phase offsets between transmit-receive oscillators or from mobility-induced Doppler effects, with the latter causing a spectrum of frequency drifts. Subcarrier drifts cause inter-carrier interference (ICI), which renders (3) invalid. On the other hand, high PAPR necessitates backing-off transmit-power amplifiers to avoid nonlinear distortion effects (Batra et al., 2004).

However, the same multipath robustness can be obtained by adopting ZP instead of CP (Lu et al., 2009). If the length of the zero-padding equals the length of CP, then the ZP-OFDM will achieve the same spectrum efficiency as CP-OFDM.

The only difference between the transmission part of the ZP-OFDM and CP-OFDM, as shown in Fig. 2, is the CP replaced by D appending zeros at the end of the symbol. If we define $\mathbf{F}_{zp} := [\mathbf{F}_M, \mathbf{0}]^H$, and $Z = C = M + D$, the transmitted OFDM symbol can be denoted as $\tilde{\mathbf{x}}_{zp,i} = \mathbf{F}_{zp} \mathbf{X}_i$. The received symbol is now expressed as:

$$\tilde{\mathbf{y}}_{zp,i} = \mathbf{H} \mathbf{F}_{zp} \mathbf{X}_i + \mathbf{H}_{ISI} \mathbf{F}_{zp} \mathbf{X}_{i-1} + \tilde{\mathbf{n}}_{Z,i}. \quad (5)$$

The key advantage of ZP-OFDM relies on two aspects: first, the all-zero $D \times M$ matrix $\mathbf{0}$ is able to take good care of the ISI, when the length of the padded zeros is not less than the maximum channel delay. Second, according to the Eq. (4), multipath channel will introduce 3 impact factors, h_l , k and l to the received signal, which stand for the amplitude, subcarriers (in frequency domain) and delay (in time domain), respectively. Therefore, different CP copies from multipath certainly pose stronger interference than ZP copies. Thus, without equalization or some pre-modulation schemes, like Differential-PSK, the ZP-OFDM has a natural better bit error rate (BER) performance than the CP-OFDM. Furthermore, the linear structure of the channel matrix in ZP-OFDM ensures the symbol recovery regardless of the channel zeros locations.

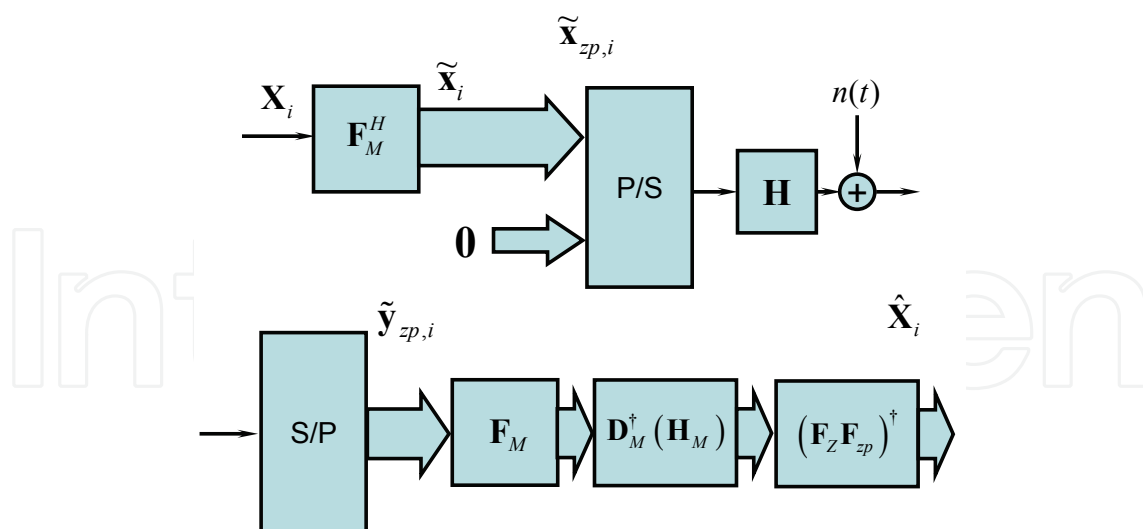


Fig. 2. Discrete-time block equivalent models of ZP-OFDM, top: transmitter & channel, bottom: receiver.

Nevertheless, because of the zero-padding and linear structure of ZP-OFDM, it outperforms CP-OFDM in terms of the lower PAPR (Batra et al., 2004; Lu et al., 2009). Similar to silent periods in TDMA, trailing zeros will not pose problems to high-power amplifiers (HPA). By adopting the proper filter, they will not give rise to out-of-band spectral leakage, either. The

circulant channel convolution matrix $\mathbf{C}_M(\mathbf{h})$ in the CP-OFDM is invertible if and only if the channel transfer function has no zeros on the FFT grid, i.e., $H_k \neq 0, \forall k \in [1, M]$, therefore, when channel nulls hit the transmitted symbols, the signal recovery becomes impossible. However, in the ZP-OFDM, the tall Toeplitz structure of equivalent channel matrix always guarantees its full rank (it only becomes rank deficient when the channel impulse response is identically zero, which is impossible in practice) (Muquet et al., 2009). In other words, the full rank property guarantees the detection of transmitted symbols.

In the blind channel estimation and blind symbol synchronization, ZP-OFDM also has its advantage in reducing the system complexity. Therefore, for more efficient utilization of the spectrum and low power transmission, a fast-equalized ZP-OFDM seems more promising than the CP-OFDM.

The above reviewed advantages and limitations of single-transceiver CP-OFDM and ZP-OFDM systems are basically present in the cooperative scenario which we present later under the name of cooperative OFDM.

1.2.2 From MIMO to cooperative communications

MIMO systems have been constructed comprising multiple antennas at both the transmitter and receiver to offer significant increases in data throughput and link range without additional expenditure in frequency and time domain. The spatial diversity has been studied intensively in the context of MIMO systems (Barbarossa, 2005). It has been shown that utilizing MIMO systems can significantly improve the system throughput and reliability (Foschini & Gans, 1998).

In the fourth generation wireless networks to be deployed in the next couple of years, namely, mobile broadband wireless access (MBWA) or IEEE 802.20, peak data rates of 260 Mbps can be achieved on the downlink, and 60 Mbps on the uplink (Hwang et al., 2007). These data rates can, however, only be achieved for full-rank MIMO users. More specifically, full-rank MIMO users must have multiple antennas at the mobile terminal, and these antennas must see independent channel fades to the multiple antennas located at the base station. In practice, not all users can guarantee such high rates because they either do not have multiple antennas installed on their small-size devices, or the propagation environment cannot support MIMO because, for example, there is not enough scattering. In the latter case, even if the user has multiple antennas installed full-rank MIMO is not achieved because the paths between several antenna elements are highly correlated.

To overcome the above limitations of achieving MIMO gains in future wireless networks, we must think of new techniques beyond traditional point-to-point communications. The traditional view of a wireless system is that it is a set of nodes trying to communicate with each other. From another point of view, however, because of the broadcast nature of the wireless channel, we can think of those nodes as a set of antennas distributed in the wireless system. Adopting this point of view, nodes in the network can cooperate together for a distributed transmission and processing of information. The cooperating node acts as a relay node for the source node. Since the relay node is usually several wavelengths distant from the source, the relay channels are guaranteed to fade independently from the direct channels, as well as each other which introduces a full-rank MIMO channel between the source and the destination. In the cooperative communications setup, there is a-priori few constraints to different nodes receiving useful energy that has been emitted by another transmitting node. The new paradigm in user cooperation is that, by implementing the appropriate signal

processing algorithms at the nodes, multiple terminals can process the transmissions overheard from other nodes and be made to collaborate by relaying information for each other. The relayed information is subsequently combined at a destination node so as to create spatial diversity. This creates a network that can be regarded as a system implementing a distributed multiple antenna where collaborating nodes create diverse signal paths for each other (Liu et al., 2009). Therefore, we study the cooperative relay communication system, and consequently, a cooperative ZP-OFDM to achieve the full diversity is investigated.

The rest of the chapter is organized as follows. In Section II, we first provide and discuss the basic models of AF, DF and their hybrid scheme. The performance analysis of the hybrid DF-AF is presented in Section III. The cooperative ZP-OFDM scheme, which will be very promising for the future cooperative Ultra Wide Band (UWB) system, is addressed in Section IV, the space time frequency coding (STFC) scheme for the full diversity cooperation is proposed as well. The conclusions of the chapter appear in Section VI.

2. System model

Cooperative communications is a new paradigm shift for the fourth generation wireless system that will guarantee high data rates to all users in the network, and we anticipate that it will be the key technology aspect in the fifth generation wireless networks (Liu et al., 2009).

In terms of research ascendance, cooperative communications can be seen as related to research on relay channel and MIMO systems. The concept of user cooperation itself was introduced in two-part series of papers (Sendonaris et al., Part I, 2003; Sendonaris et al., Part II, 2003). In these works, Sendonaris *et al.* proposed a two-user cooperation system, in which pairs of terminals in the wireless network are coupled to help each other forming a distributed two-antenna system. Cooperative communications allows different users or nodes in a wireless network to share resources and to create collaboration through distributed transmission/processing, in which each user's information is sent out not only by the user but also by the collaborating users (Nosratinia et al., 2004). Cooperative communications promises significant capacity and multiplexing gain increase in the wireless system (Kramer et al., 2005). It also realizes a new form of space diversity to combat the detrimental effects of severe fading. There are mainly two relaying protocols: AF and DF.

2.1 Amplify and forward protocol

In AF, the received signal is amplified and retransmitted to the destination. The advantage of this protocol is its simplicity and low cost implementation. But the noise is also amplified at the relay. The AF relay channel can be modeled as follows. The signal transmitted from the source x is received at both the relay and destination as

$$y_{S,r} = \sqrt{E_S} h_{S,r} x + n_{S,r}, \text{ and } y_{S,D} = \sqrt{E_S} h_{S,D} x + n_{S,D} \quad (6)$$

where $h_{S,r}$ and $h_{S,D}$ are the channel gains between the source and the relay and destination, respectively, and are modeled as Rayleigh flat fading channels. The terms $n_{S,r}$ and $n_{S,D}$ denote the additive white Gaussian noise with zero-mean and variance N_0 , E_S is the average transmission energy at the source node. In this protocol, the relay amplifies the signal from the source and forwards it to the destination ideally to equalize the effect of the channel

fading between the source and the relay. The relay does that by simply scaling the received signal by a factor A_r that is inversely proportional to the received power, which is denoted by

$$A_r = \sqrt{\frac{E_s}{E_s h_{s,r} + N_0}} \quad (7)$$

The destination receives two copies from the signal x through the source link and relay link. There are different techniques to combine the two signals at the destination. The optimal technique that maximizes the overall SNR is the maximal ratio combiner (MRC). Note that the MRC combining requires a coherent detector that has knowledge of all channel coefficients, and the SNR at the output of the MRC is equal to the sum of the received signal-to-noise ratios from all branches.

2.2 Decode and forward protocol

Another protocol is termed as a decode-and-forward scheme, which is often simply called a DF protocol. In the DF, the relay attempts to decode the received signals. If successful, it re-encodes the information and retransmits it. Although DF protocol has the advantage over AF protocol in reducing the effects of channel interferences and additive noise at the relay, the system complexity will be increased to guarantee the correct signal detection.

Note that the decoded signal at the relay may be incorrect. If an incorrect signal is forwarded to the destination, the decoding at the destination is meaningless. It is clear that for such a scheme the diversity achieved is only one, because the performance of the system is limited by the worst link from the source-relay and source-destination (Laneman et al., 2004).

Although DF relaying has the advantage over AF relaying in reducing the effects of noise and interference at the relay, it entails the possibility of forwarding erroneously detected signals to the destination, causing error propagation that can diminish the performance of the system. The mutual information between the source and the destination is limited by the mutual information of the weakest link between the source-relay and the combined channel from the source-destination and relay-destination.

Since the reliable decoding is not always available, which also means DF protocol is not always suitable for all relaying situations. The tradeoff between the time-consuming decoding, and a better cooperative transmission, finding the optimum hybrid cooperative schemes, that include both DF and AF for different situations, is an important issue for the cooperative wireless networks design.

2.3 Hybrid DF-AF protocol

In this chapter, we consider a hybrid cooperative OFDM strategy as shown in Fig. 3, where we transmit data from source node S to destination node D through R relays, without the direct link between S and D . This relay structure is called 2-hop relay system, i.e., first hop from source node to relay, and second hop from relay to destination. The channel fading for different links are assumed to be identical and statistically independent, quasi-statistic, i.e., channels are constant within several OFDM symbol durations. This is a reasonable assumption as the relays are usually spatially well separated and in a slow changing environment. We assume that the channels are well known at the corresponding receiver

sides, and a one bit feedback channel from destination to relay is used for removing the unsuitable AF relays. All the AWGN terms have equal variance N_0 . Relays are re-ordered according to the descending order of the SNR between S and Q , i.e., $\text{SNR}_{SQ_1} > \dots > \text{SNR}_{SQ_R}$, where SNR_{SQ_r} denotes the r -th largest SNR between S and Q .

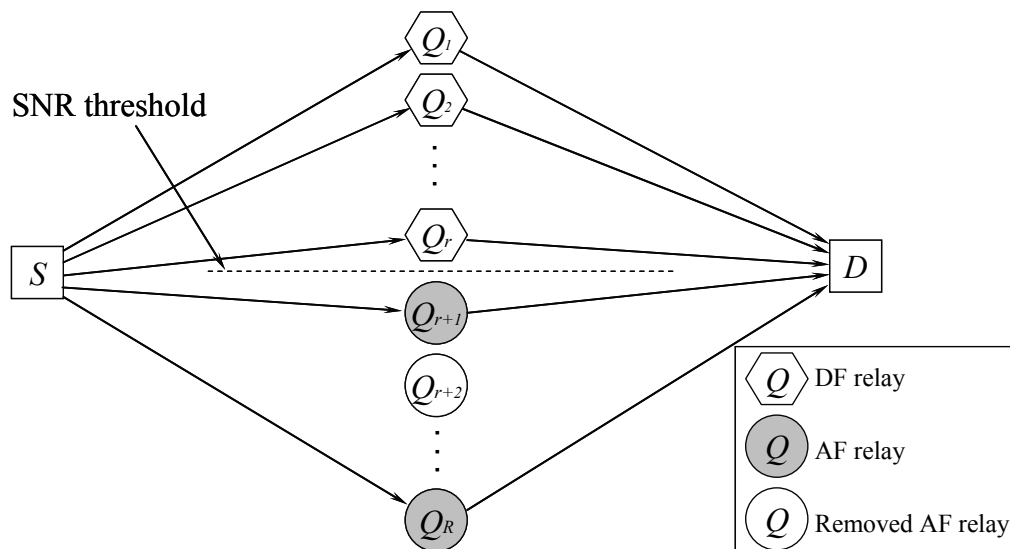


Fig. 3. Hybrid relay cooperation with dynamic optimal combination of DF-AF relays (S: Source, D: Destination, Q_r : r -th Relay)

In this model, relays can determine whether the received signals are decoded correctly or not, just simply by comparing the SNR to the threshold, which will be elaborated in Section 3.1. Therefore, the relays with SNR above the threshold will be chosen to decode and forward the data to the destination, as shown with the white hexagons in Fig.3. The white circle is the removed AF relay according to the dynamic optimal combination strategy which will be proposed in Section 3.2. The rest of the relays follow the AF protocol, as shown with the white hexagons in Fig. 3 (Lu & Nikookar, 2009; Lu et al., 2010).

The received SNR at the destination in the hybrid cooperative network can be denoted as

$$\gamma_h = \sum_{Q_i \in \text{DF}} \frac{E_Q h_{Q_i, D}}{N_0} + \sum_{Q_j \in \text{AF}} \frac{\frac{E_S h_{S, Q_j}}{N_0} \frac{E_Q h_{Q_j, D}}{N_0}}{\frac{E_S h_{S, Q_j}}{N_0} + \frac{E_Q h_{Q_j, D}}{N_0} + 1} \quad (8)$$

where $h_{Q_i, D}$, h_{S, Q_j} and $h_{Q_j, D}$ denote the power gains of the channel from the i -th relay to the destination in DF protocol, source node to the j -th relay in AF protocol and j -th relay to the destination in AF protocol, respectively. E_S and E_Q in (8) are the average transmission energy at the source node and at the relays, respectively. By choosing the amplification factor A_{Q_j} in the AF protocol as:

$$A_{Q_j}^2 = \frac{E_S}{E_S h_{S, Q_j} + N_0} \quad (9)$$

and forcing the E_Q in DF equal to E_s , it will be convenient to maintain constant average transmission energy at relays, equal to the original transmitted energy at the source node. In this chapter, OFDM is used as a modulation technique in the cooperative system to gain from its inherent advantages and combat frequency selective fading of each cooperative link, with W_r , $r = 1, 2, \dots, R$ independent paths. Later, we also show that, by utilizing the space-frequency coding, hybrid DF-AF cooperative OFDM can also gain from the frequency selective fading and achieve the multi-path diversity with a diversity gain of $W_{min} = \min(W_r)$. As shown in the Fig.4, the r -th relay first decides to adopt DF or AF protocol according to the SNR threshold. For the DF-protocol, the symbols are decoded at the relays, and then an IFFT operation is applied on these blocks to produce the OFDM symbol. Before transmission, a prefix (CP or ZP) is added to each OFDM symbol. For the AF-protocol, relays which undergo the deep fading will be removed by using the dynamic optimal combination strategy discussed later in this section. Other AF relays are proper relays, amplify and forward the data to the destination. At the destination node, after the prefix removal, the received OFDM symbols are fast-Fourier-transformed, and the resulting symbols at the destination are used for the combination and detection.

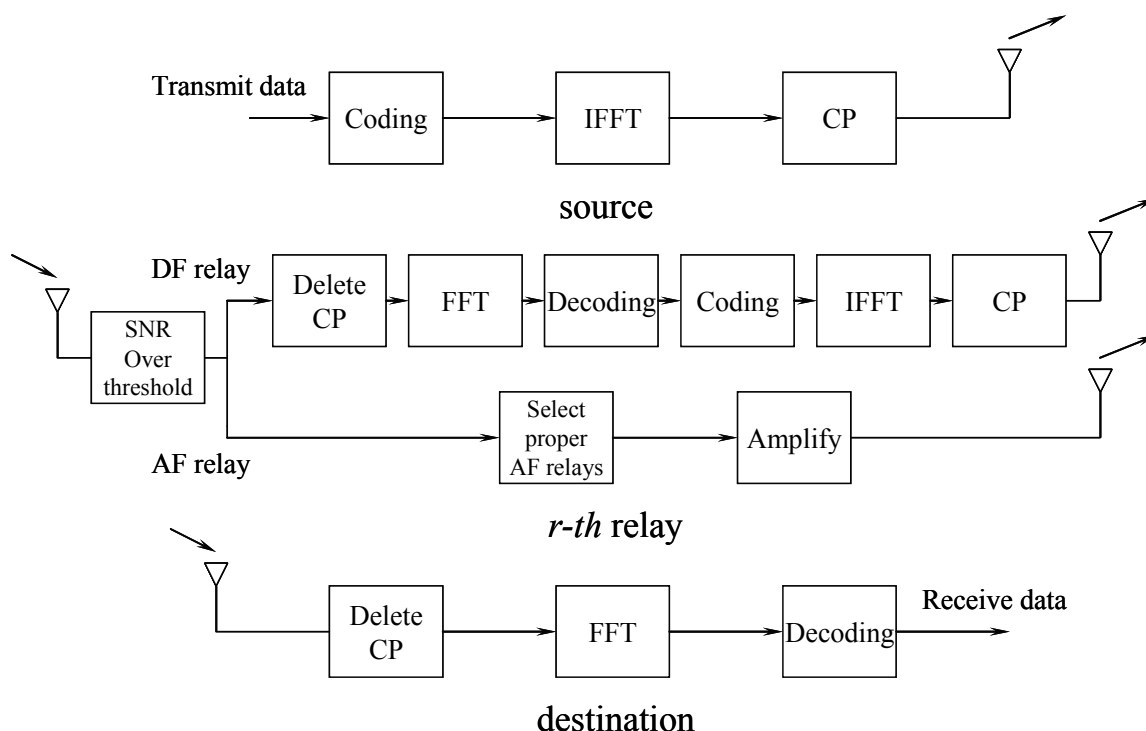


Fig. 4. Relay selection in the hybrid DF-AF cooperative OFDM wireless transmission strategy (top: source, middle: relay, bottom: destination)

The receiver at the destination collects the data from DF and AF relays with a MRC. Because of the amplification in the intermediate stage in the AF protocol, the overall channel gain of the AF protocol should include the source to relay, relay to destination channels gains and amplification factor. The decision variable u at the MRC output is given by

$$u = \sum_{Q_i \in \text{DF}} \frac{(H_{Q_i,D})^* Y_{Q_i}}{(H_{Q_i,D})^* H_{Q_i,D}} + \sum_{Q_j \in \text{AF}} \frac{(H_{S,Q_j} A_{Q_j} H_{Q_j,D})^* Y_{Q_j}}{(H_{S,Q_j} A_{Q_j} H_{Q_j,D})^* (H_{S,Q_j} A_{Q_j} H_{Q_j,D})} \quad (10)$$

where Y_{Q_i} and Y_{Q_j} are the received signal from DF i -th relay and AF j -th relays, respectively, and $(\cdot)^*$ denotes the conjugate operation. $H_{Q_i,D}$, H_{S,Q_i} and $H_{Q_j,D}$ are frequency response of the channel power gains, respectively.

In the proposed hybrid DF-AF cooperative network, DF plays a dominant role in the whole system. However, switching to AF scheme for the relay nodes with SNR below the threshold often improves the total transmission performance, and accordingly AF plays a positive compensating role.

3. Performance analysis of Hybrid DF-AF protocol

3.1 Threshold for DF and AF relays

In general, mutual information I is the upper bound of the target rate B bit/s/Hz, i.e., the spectral efficiency attempted by the transmitting terminal. Normally, $B \leq I$, and the case $B > I$ is known as the outage event. Meanwhile, channel capacity, C , is also regarded as the maximum achievable spectral efficiency, i.e., $B \leq C$.

Conventionally, the maximum average mutual information of the direct transmission between source and destination, i.e., I_D , achieved by independent and identically distributed (i.i.d) zero-mean, circularly symmetric complex Gaussian inputs, is given by

$$I_D = \log_2(1 + \text{SNR } h_{S,D}) \quad (11)$$

as a function of the power gain over source and destination, $h_{S,D}$. According to the inequality $B \leq I$, we can derive the SNR threshold for the full decoding as

$$\text{SNR} \geq \frac{2^B - 1}{h_{S,D}} \quad (12)$$

Then, we suppose all of the X relays adopt the DF cooperative transmission without direct transmission. The maximum average mutual information for DF cooperation I_{DF_co} is shown (Laneman et al., 2004) to be

$$I_{DF_co} = \frac{1}{X} \min \left\{ \log_2 \left(1 + \sum_{r=1}^R \text{SNR } h_{S,Q_r} \right), \log_2 \left(1 + \sum_{r=1}^R \text{SNR } h_{Q_r,D} \right) \right\} \quad (13)$$

which is a function of the channel power gains. Here, R denotes the number of the relays. For the r -th DF link, requiring both the relay and destination to decode perfectly, the maximum average mutual information I_{DF_li} can be shown as

$$I_{DF_li} = \min \left\{ \log_2 (1 + \text{SNR } h_{S,Q_r}), \log_2 (1 + \text{SNR } h_{Q_r,D}) \right\} \quad (14)$$

The first term in (14) represents the maximum rate at which the relay can reliably decode the source message, while the second term in (14) represents the maximum rate at which the destination can reliably decode the message forwarded from relay. We note that such mutual information forms are typical of relay channel with full decoding at the relay (Cover & El Gamal, 1979). The SNR threshold of this DF link for target rate B is given by $I_{DF_li} \geq B$ which is derived as

$$\text{SNR} \geq \frac{2^B - 1}{\min(h_{S,Q_r}, h_{Q_r,D})} \quad (15)$$

In the proposed hybrid DF-AF cooperative transmission, we only consider that a relay can fully decode the signal transmitted over the source-relay link, but not the whole DF link. Thus, the SNR threshold for the full decoding at the r -th relay reaches its lower bound as

$$\gamma_{th} \geq \frac{2^B - 1}{h_{S,Q_r}} \quad (16)$$

For the DF protocol, let R denote the number of the total relays, M denote the set of participating relays, whose SNRs are above the SNR threshold, and the reliable decoding is available. The achievable channel capacity, C_{DF} , with SNR threshold is calculated as

$$C_{DF} = \sum_M \frac{1}{R} \mathbf{E}(\log_2(1 + y|M)) \Pr(M) \quad (17)$$

where $\mathbf{E}(\cdot)$ denotes the expectation operator, $y|M = (R - K)\gamma_{S,D} + \sum_{Q \in M} \gamma_{Q,D}$ denotes the instantaneous received SNR at the destination given set M with K participating relays, where $\gamma_{n,m}$ denotes the instantaneous received SNR at node m , which is directly transmitted from n to m . Since $y|M$ is the weighted sum of independent exponential random variables (Farhadi & Beaulieu, 2008), the probability density function (PDF) of $y|M$ can be obtained using its moment generating function (MGF) and partial fraction technique for evaluation of the inverse Laplace transform, see Eq. (8d) and Eq. (8e) in (Farhadi & Beaulieu, 2008). $\Pr(M)$ in (17) is the probability of a particular set of participating relays which are obtained as

$$\Pr(M) = \prod_{Q \in M} \exp\left(-\frac{R\gamma_{th}}{\Gamma_{S,Q \in M}}\right) \prod_{Q \notin M} \left(1 - \exp\left(-\frac{R\gamma_{th}}{\Gamma_{S,Q \notin M}}\right)\right) \quad (18)$$

where $\Gamma_{u,v}$ denotes the average SNR over the link between nodes u and v .

Combining (13), (17) and (18) with the inequality $I_{DF_co} \leq C_{DF}$, since the maximum average mutual information, I , is upper bound by the achievable channel capacity, C , we can calculate the upper bound of SNR threshold γ_{th} for fully decoding in the DF protocol.

Now, we can obtain the upper bound and the lower bound of the SNR threshold γ_{th} for the hybrid DF-AF cooperation. However, compared to the upper bound, the lower bound as shown in the (16) is more crucial for improving the transmission performance. This is because the DF protocol plays a dominant role in the hybrid cooperation strategy, and accordingly we want to find the lower bound which provides as much as possible DF relays. We will elaborate this issue later. Fully decoding check can also be guaranteed by employing the error detection code, such as cyclic redundancy check. However, it will increase the system complexity (Lin & Costello, 1983).

3.2 Dynamic optimal combination scheme

In the maximum ratio combining the transmitted signal from R cooperative relays nodes, which underwent independent identically distributed Rayleigh fading, and forwarded to

the destination node are combined. In this case the SNR per bit per relay link γ_r has an exponential probability density function (PDF) with average SNR per bit $\bar{\gamma}$:

$$p_{\gamma_r}(\gamma_r) = \frac{1}{\bar{\gamma}} e^{-\gamma_r/\bar{\gamma}} \quad (19)$$

Since the fading on the R paths is identical and mutually statistically independent, the SNR per bit of the combined SNR γ_c will have a Chi-square distribution with $2R$ degrees of freedom. The PDF $p_{\gamma_c}(\gamma_c)$ is

$$p_{\gamma_c}(\gamma_c) = \frac{1}{(R-1)! \bar{\gamma}_c^R} \gamma_c^{R-1} e^{-\gamma_c/\bar{\gamma}_c} \quad (20)$$

where $\bar{\gamma}_c$ is the average SNR per channel, then by integrating the conditional error probability over $\bar{\gamma}_c$, the average probability of error P_e can be obtained as

$$P_e = \int_0^\infty \mathbb{Q}(\sqrt{2g\gamma_c}) p_{\gamma_c}(\gamma_c) d\gamma_c \quad (21)$$

where $g = 1$ for coherent BPSK, $g = 1/2$ for coherent orthogonal BFSK, $g = 0.715$ for coherent BFSK with minimum correlation, and $\mathbb{Q}(\cdot)$ is the Gaussian Q-function, i.e., $\mathbb{Q}(x) = 1/\sqrt{2\pi} \int_x^\infty \exp(-t^2/2) dt$. For the BPSK case, the average probability of error can be found in the closed form by successive integration by parts (Proakis, 2001), i.e.,

$$P_e = \left(\frac{1-\mu}{2}\right)^R \sum_{k=0}^{R-1} \binom{R-1+k}{k} \left(\frac{1+\mu}{2}\right)^R \quad (22)$$

where

$$\mu = \sqrt{\frac{\bar{\gamma}_c}{1+\bar{\gamma}_c}} \quad (23)$$

In the hybrid DF-AF cooperative network with two hops in each AF relay, the average SNR per channel $\bar{\gamma}_c$ can be derived as

$$\bar{\gamma}_c = \frac{\gamma_h}{K+2 \times J} \quad (24)$$

where K and J are the numbers of the DF relays and AF relays, respectively. γ_h can be obtained from (8). In the DF protocol, due to the reliable detection, we only need to consider the last hops, or the channels between the relay nodes and destination node.

As the average probability of error P_e is a precise indication for the transmission performance, we consequently propose a dynamic optimal combination strategy for the hybrid DF-AF cooperative transmission. In this algorithm the proper AF relays are selected to make P_e reach maximum.

First of all, like aforementioned procedure, relays are reordered according to the descending order of the SNR between source and relays, as shown in the Fig.3. According to the proposed SNR threshold, we pick up the DF relays having SNR greater than threshold. Then, we proceed with the AF relay selection scheme, where the inappropriate AF relays are removed. The whole dynamic optimal combination strategy for the hybrid DF-AF cooperation is shown in the flow chart of Fig. 5.

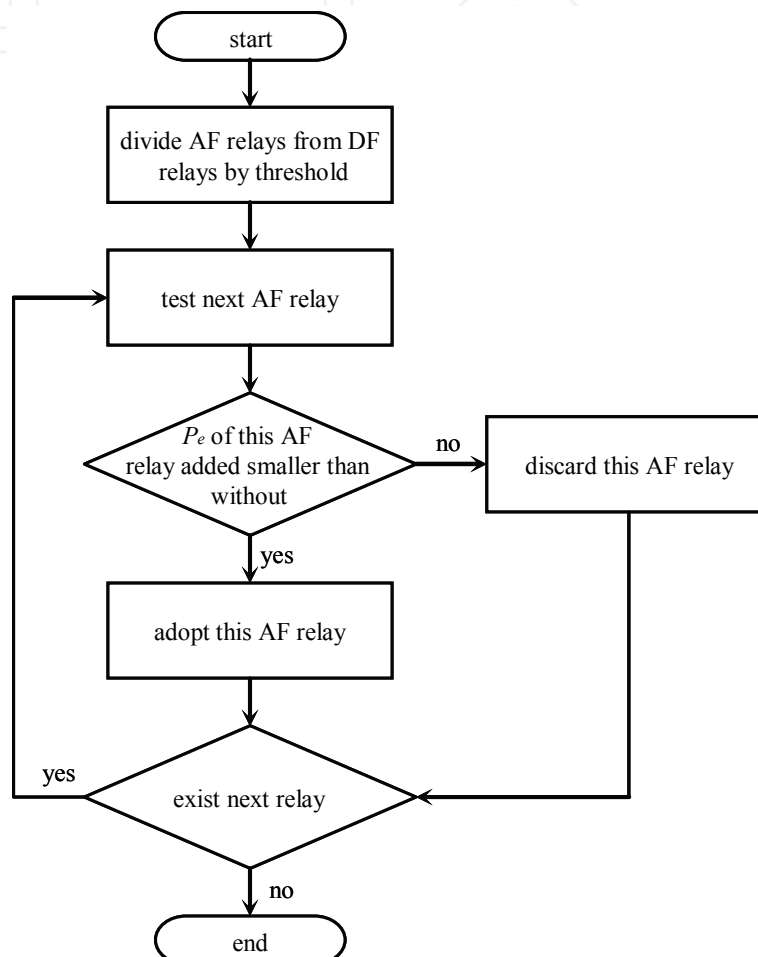


Fig. 5. Flow chart of the dynamic optimal combination strategy for the hybrid DF-AF cooperation

By exploiting the space-frequency coding proposed in (Li et al., 2009), we can further gain from the hybrid DF-AF cooperative OFDM in the frequency selective channel by coding across relays and OFDM tones, and obtain the multi-path diversity. According to the Eq. (14) in (Li et al., 2009), the multi-path diversity of the hybrid DF-AF cooperative OFDM can be shown by the upper bound of the error probability as:

$$\begin{aligned}
 P_e &< G_c^{-RW_{\min}} \left(\frac{\log \gamma_h}{\gamma_h} \right)^{RW_{\min}} \\
 &\approx (G_c \gamma_h)^{-RW_{\min}} \text{ as } \gamma_h \rightarrow \infty
 \end{aligned} \tag{25}$$

where G_c is a constant, which can be shown as Eq. (35) in (Li et al., 2009), γ_h is the average SNR at the destination in the hybrid cooperative network, and can be calculated by (8) in this chapter.

It can be seen from (25) that the achievable diversity gain is RW_{min} , i.e., the product of the cooperative (relay) diversity R and the multi-path diversity W_{min} . Here $W_{min} = \min (W_r)$, where $W_r, r = 1, 2, \dots, R$ is the number of independent paths in each relay-destination link.

3.3 Simulation results

First, we simulated BPSK modulation, Rayleigh channel, flat fading, without OFDM, and supposed the SNR threshold for correct decoding is $4E_b/N_0$, then we assumed $h_{Q_i,D} = h_{S,Q_j} = h_{Q_j,D} = 1$, for all branches, to verify proposed analytical BER expression. The resulting average BERs were plotted against the transmit SNR defined as $SNR = E_b/N_0$. As shown in the Fig. 6, the theoretical curves of multi-DF cooperation derived from our analytical closed-form BER expression clearly agree with the Monte Carlo simulated curves, while the theoretical curves of 2-AF and 3-AF cooperation match the simulation result only at the low SNR region.

Fig. 7 shows the BER performance for hybrid DF-AF cooperation. For the DF-dominant hybrid cooperation, the theoretical curves exhibit a good match with the Monte Carlo simulation results curves. The slight gap between theoretical and simulation BER results for the hybrid case of 1-DF + multi-AF can be explained by the AF relay fading which was considered as a double Gaussian channel, a product of two complex Gaussian channel (Patel et al., 2006). Obviously, the distribution of combined SNR (i.e., γ_c) will no longer follow the chi-square distribution giving rise to this slight difference.

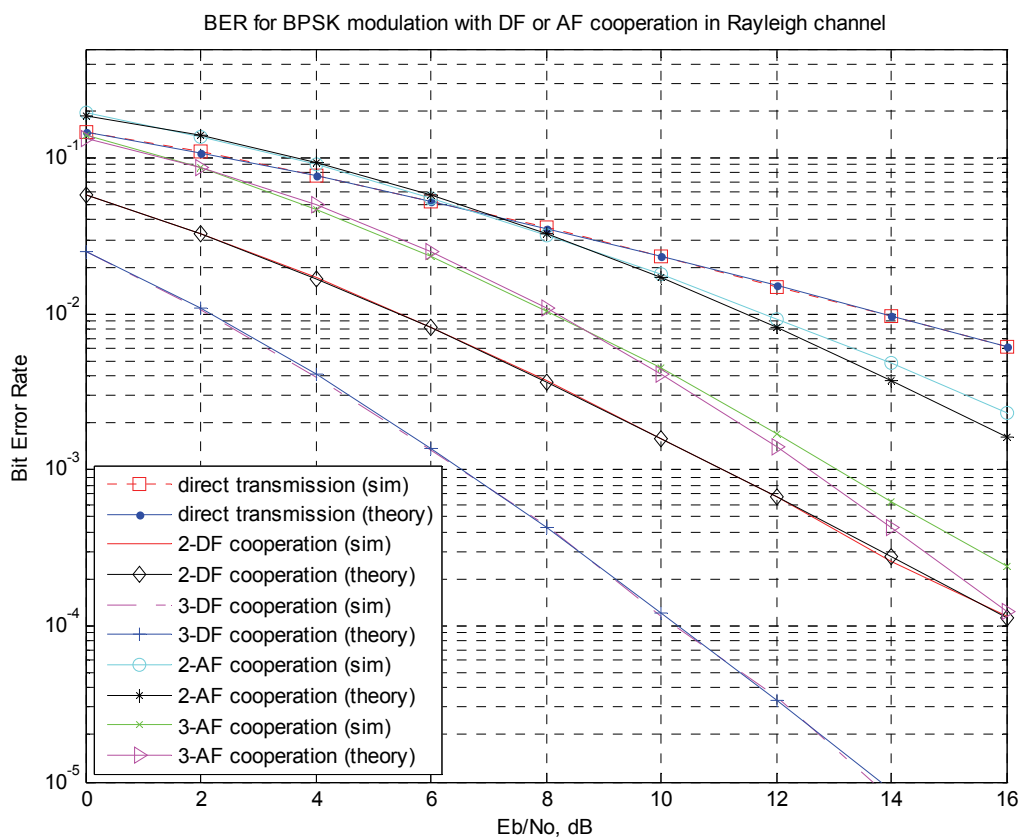


Fig. 6. BER performance for DF or AF cooperation.

In this proposed hybrid cooperation protocol, DF is dominant. We show this characteristic of the hybrid DF-AF cooperation by the following theorem:

Theorem 1: For the F -hop relay link, and the full decoding in DF protocol, as long as the SNR of the last hop is larger than $1/F$ times of the arithmetic mean of the whole link SNR, DF always plays a more important role than AF in improving the BER performance.

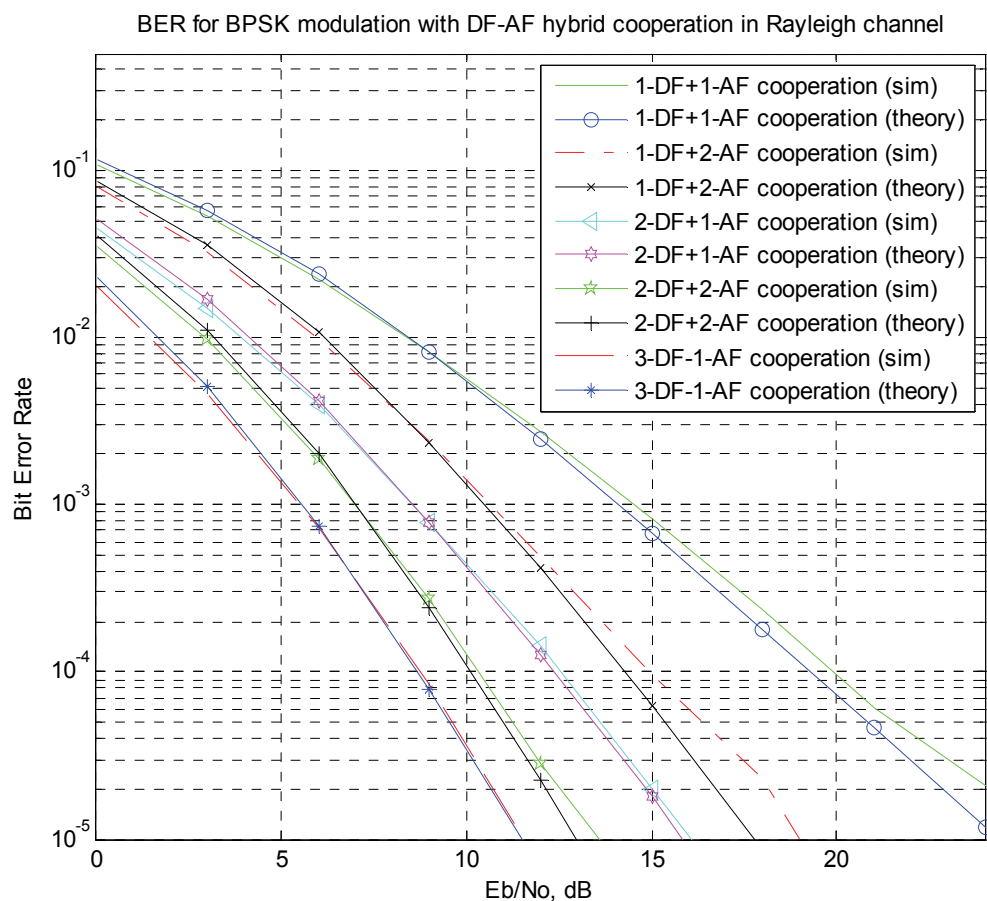


Fig. 7. BER performance for hybrid DF+AF cooperation.

Proof: According to the (22) and (23), the average probability of error P_e is a decreasing function w.r.t. combined SNR, γ_c . The SNR of the F -hop AF relay link, γ_{AF} , is the $1/F$ times of the harmonic mean of $\gamma_i, \forall i \in [1, F]$, i.e. (Hasna & Alouini, 2002),

$$\gamma_{AF} = \frac{\gamma_1 \gamma_2 \dots \gamma_L}{\sum_{i=1}^L \gamma_1 \gamma_2 \dots \gamma_{i-1} \gamma_{i+1} \dots \gamma_L} \quad (26)$$

Using Pythagorean means theorem, the harmonic mean is always smaller than the arithmetic mean. ■

For instance, in the high SNR region, the second term of (8) can be approximated as the $1/2$ times the harmonic mean of the 2-hop SNR in AF relay link (i.e., 1 is negligible in the denominator). As in practice, it is very easy for the last hop relay to achieve a SNR larger than $1/L$ times of the arithmetic mean of the whole link SNR, we can only consider the last hop of the reliably decoded DF protocol. Therefore, under the condition of the correct decoding, DF can enhance the error probability performance better than AF in the cooperative relay network.

This DF dominant hybrid cooperative networks strategy can be verified by the above simulation results as well. Comparing 2-DF to 2-AF in Fig. 6, or 2-DF plus 1-AF to 1-DF plus 2-AF in Fig. 7, or other hybrid DF-AF protocols with the same R , we can see that the fully decoded DF protocols always show a better BER performance than AF protocols. Therefore, DF protocols with a reliable decoding play a more important role in hybrid cooperative networks than AF protocols. Meanwhile, we can see from the figure that, changing to the AF scheme for the relay nodes with SNR below the threshold also improves the BER performance, as well as the diversity gain of the whole network. In fact, this is a better way than just discarding these relay nodes.

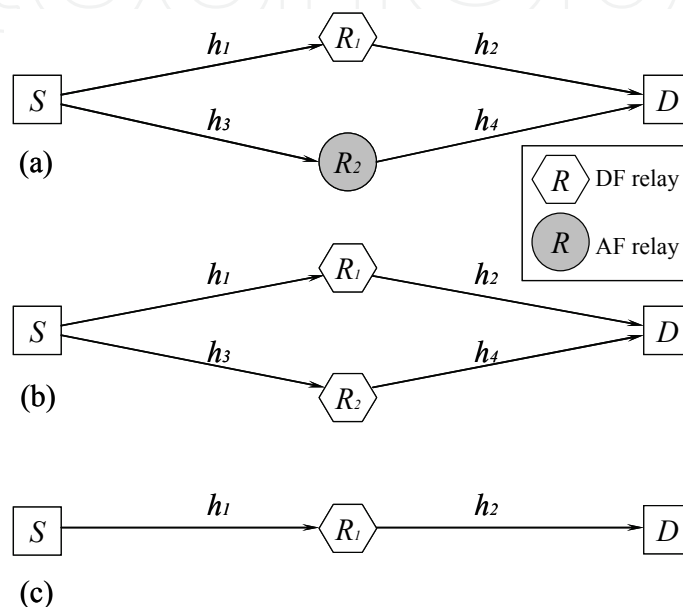


Fig. 8. hybrid DF-AF cooperation and DF cooperation architectures with different average power gains. (a) hybrid DF-AF cooperation, (b) dual DF cooperation, (c) single DF cooperation. (S : Source, D : Destination, h : average power gain between two nodes).

Reference (Louie et al., 2009) proposes a closed-form BER expression for two-hop AF protocol, which includes Gauss' hypergeometric and Gamma functions. This closed-form BER expression needs more computational burden to derive the cooperative analytical expression. In (Sadek et al., 2007), the analytical expression for multi-node DF protocol is provided with a complicated form as well. Instead, the compact closed-form BER expression for hybrid DF-AF cooperation proposed in this chapter allows us to achieve insight into the results with relatively low computations. The simple expressions can also help understanding the factors affecting the system performance. It can also be used for designing different network functions such as power allocation, scheduling, routing, and node selection.

In order to study the effect of the channel gains between source, relay and destination, we compare the hybrid DF-AF with the dual DF as well as the single DF cooperation in Fig. 8. In this figure, h_1 , h_2 , h_3 and h_4 stand for the average power gain between corresponding two nodes. In this simulation, the SNR threshold for correct decoding is assumed to be $4E_b/N_0$, and we set the first hop average power gain in DF protocol, i.e., h_1 in Fig. 8 (a) and Fig. 8 (c), and h_1 , h_3 in Fig. 8 (b) as 4, which means that the relay in DF protocol can fully decode the signal. The average power gains of the first hop in AF protocol, i.e., h_3 in Fig. 8 (a) increases

from 0.25 to 20. It can be seen from the Fig. 9 that the dual DF cooperation with reliable decoding outperforms the hybrid DF-AF cooperation, when corresponding average power gains are the same, i.e., diamond marked curve is better than square marked curve in Fig. 9. Meanwhile, the comparison of the curves shows that, the AF relay which undergoes the deep fading deteriorates the BER performance of hybrid DF-AF cooperation in the low SNR region. Thus, this AF relay should be removed according to the proposed dynamic optimal combination strategy to improve the transmission performance. Sum up the above discussion, due to power control, long transmission range, serious attenuation, etc., high SNR at relay and full decoding for DF protocol is not always available. In this case, relays can change to AF protocol with enough SNR to gain from the cooperative diversity.

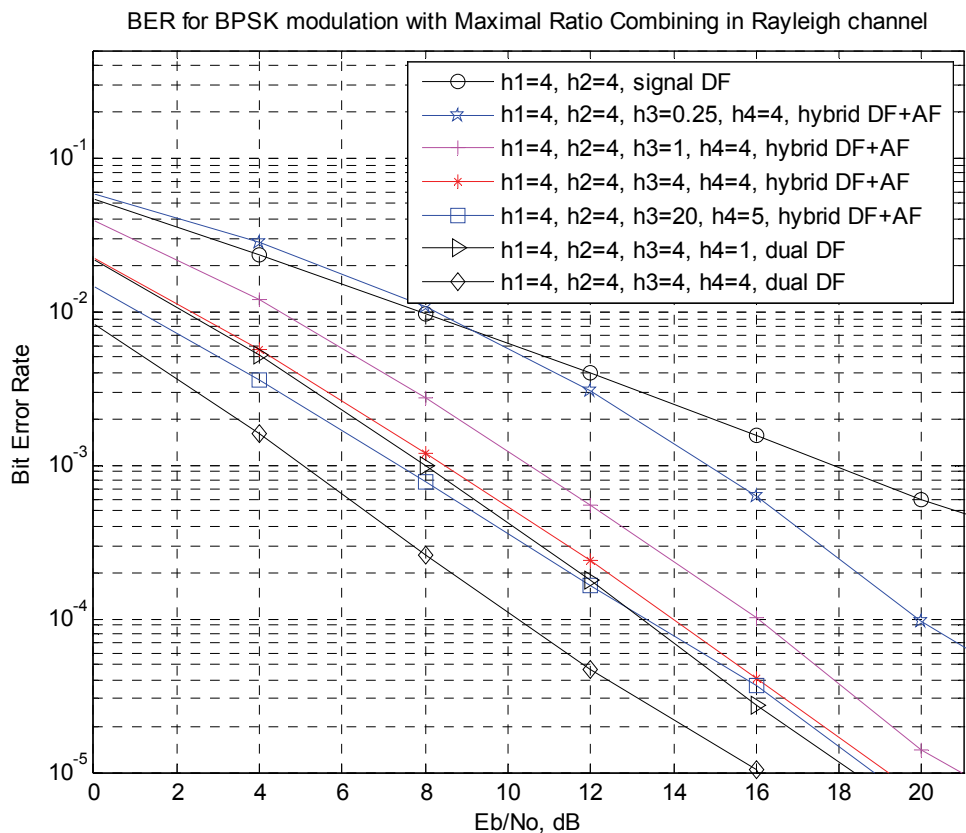


Fig. 9. BER performance for hybrid DF-AF cooperation and DF cooperation with different path gains.

Finally, we illustrate the validity of the theoretical results for the OFDM cooperation via simulations. An OFDM system with 64-point FFT and a CP length of 16 samples, which accounts for 25% of the OFDM symbol was considered. In the simulation, a more practical scenario was considered with a 3-path Rayleigh fading between each source node and relay node or relay node and destination node, i.e., $W_r = 3$. The 3-path delays were assumed at 0, 1, 2 samples, respectively. As illustrated in the Fig. 10, OFDM with CP can nicely cope with the multi-path, and the theoretical curves derived from (22) clearly agree with the Monte Carlo simulation curves. The simulation results indicate that under the condition of ISI resolved by OFDM and reliable decoding, the cooperative diversity gains from the increasing R , which is also shown by (8).

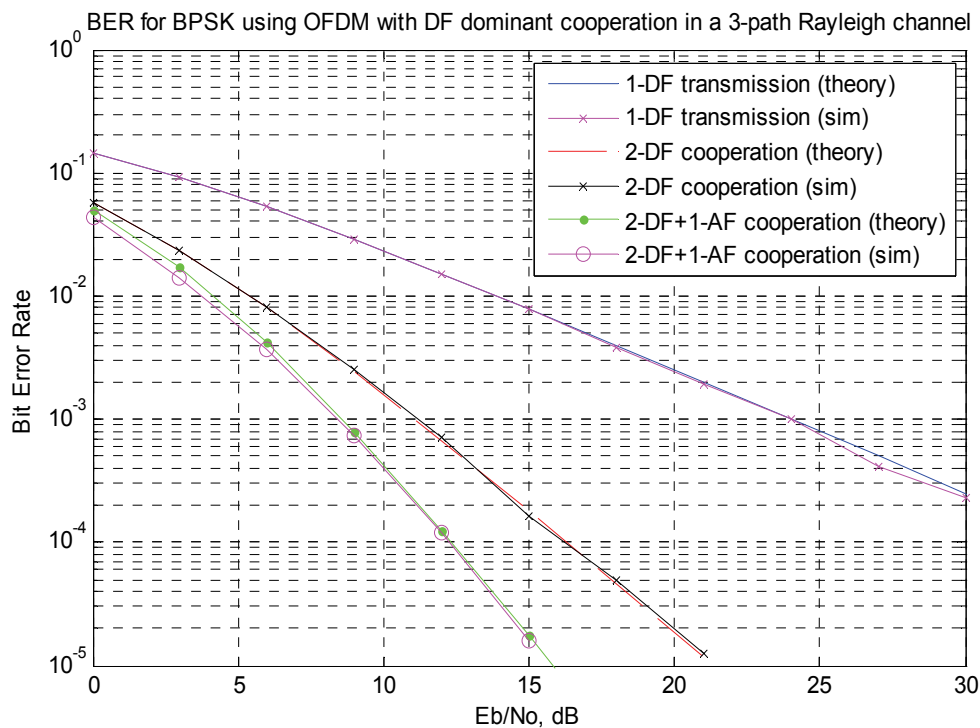


Fig. 10. BER performance for DF dominant OFDM cooperation.

4. ZP-OFDM with cooperative relays

4.1 CP and ZP for cooperative OFDM

Among the many possible multicarrier modulation techniques, OFDM is the one that has gained more acceptance as the modulation technique for high-speed wireless networks and 4G mobile broadband standards. Conventionally, CP is exploited to eliminate inter-symbol-interference (ISI) due to multipath. With a cyclic extension, the linear convolution channel is transformed into a circular convolution channel, and the ISI can be easily resolved. However, the cyclic prefix is not the only solution to combat the multipath. ZP has been recently proposed as an alternative to the CP in OFDM transmissions and Cognitive Radio (Lu et al., 2009). One of the advantages of using a ZP is that the transmitter requires less power back-off at the analog amplifier. Since the correlation caused by the cyclic prefix creates discrete spectral lines (ripples) into the average power spectral density of the transmitted signal and the radio emission power levels are limited by the Federal Communications Commission (FCC), the presence of any ripples in the power spectrum density (PSD) requires additional power back-off at the transmitter. In fact, the amount of power back-off that is required is equal to the peak-to-average ratio of the PSD.

A multiband (MB) ZP OFDM-based approach to design UWB transceivers has been recently proposed in (Batra et al., 2004) and (Batra, 2004) for the IEEE Standard. In Dec. 2008, the European Computer Manufacturers Association (ECMA) adopted ZP-OFDM for the latest version of High rate UWB Standard (Standard ECMA-368, 2008). Because of its advantage in the low power transmission, ZP-OFDM will have the potential to be used in other low power wireless communications systems.

We know that the multiple transmissions in the cooperative system may not be either time or frequency synchronized, i.e., signals transmitted from different transmitters arrive at the

receiver as different time instances, and multiple carrier frequency offsets (CFOs) also exist due to the oscillator mismatching. Different from the conventional MIMO system, the existence of multiple CFOs in the cooperative systems makes the direct CFOs compensation hard if not impossible. Therefore, in this section, we will investigate the cooperative ZP-OFDM system with multipath channel and CFOs, a subject that has not been addressed before. We propose a STFC, to hold the linear structure of the ZP-OFDM, and achieve the full cooperative spatial diversity, i.e., full multi-relay diversity. Furthermore, we show that, with only *linear receivers*, such as zero forcing (ZF) and minimum mean square error (MMSE) receivers, the proposed code achieves full diversity.

4.2 Full cooperative diversity with linear equalizer

4.2.1 Fundamental limits of diversity with linear equalizer

To quantify the performance of different communication systems, two important criteria are the average bit-error rates (BERs) and capacity. The BER performance of wireless transmissions over fading channels is usually quantified by two parameters: diversity order and coding gain (Liu et al., 2003; Tse & Viswanath, 2005). The diversity order is defined as the asymptotic slope of the BER versus signal-to-noise ratio (SNR) curve plotted in log-log scale. It describes how fast the error probability decays with SNR, while the coding gain measures the performance gap among different schemes when they have the same diversity. The higher the diversity, the smaller the error probability at high-SNR regimes. To cope with the deleterious effects of fading on the system performance, diversity-enriched transmitters and receivers have well-appreciated merits. Reference (Ma & Zhang, 2008) reveals the relationship between the channel orthogonality deficiency (*od*) and system full diversity. The orthogonality deficiency (*od*) indicates the degree of difficulty for the signal detection in the certain transceiver and channel condition (the smaller *od*, the easier signal detection). References (Shang & Xia, 2007; Shang & Xia, 2008) provide the two conditions for linear equalizer to achieve the full diversity. We will illustrate in this Section how to design the STFC to achieve full diversity for ZP-OFDM system.

In addition to focusing on diversity performance, practical systems also give high priority to reducing receiver complexity. Although maximum likelihood equalizer (MLE) enjoys the maximum diversity performance, its exponential decoding complexity makes it infeasible for certain practical systems. Some near-ML schemes (e.g., sphere decoding) can be used to reduce the decoding complexity. However, at low SNR or when large decoding blocks are sent/or high signal constellations are employed, the complexity of near-ML schemes is still high. In addition, these near-ML schemes adopt linear equalizers as preprocessing steps. To further reduce the complexity, when the system model is linear, one may apply linear equalizers (LEs) (Ma & Zhang, 2008).

4.2.2 System model and Linear ZP-OFDM

We consider a cooperative ZP-OFDM system as shown in the Fig. 11. Here the DF protocol is adopted in the cooperative communication model. Relays can fully decode the information, and participate in the cooperation, and occupy different frequency bands to transmit data to the destination. Each relay-destination link undergoes multipath Rayleigh fading. For the relay r , $r \in [1, 2, \dots, R]$, R is the number of relays, the received signal \mathbf{y}_r can be formulated as

$$\mathbf{y}_r = \mathbf{F}_{P,r} \mathbf{D}_{P,r} \mathbf{H}_r \mathbf{T}_{ZP} \mathbf{F}_{N,r}^H \mathbf{x}_r + \mathbf{n} \quad (27)$$

where $\mathbf{x}_r \triangleq [x_0, \dots, x_{N-1}]^T$ is the vector of the so called frequency transmitted information signal, and N is the signal length. The subscript r here indicates the variables or operators related to the r -th relay. To simplify the exposition, we only consider the effect of CFOs on signal. The noise term is denoted as \mathbf{n} , which stands for i.i.d. complex white Gaussian noise with zero mean. $\mathbf{F}_{N,r}$ stands for the N -point FFT matrix with (m, k) -th entry $\exp(j2\pi mk / N) / \sqrt{N}$, while $\mathbf{F}_{P,r}$ stands for the P -point FFT matrix.

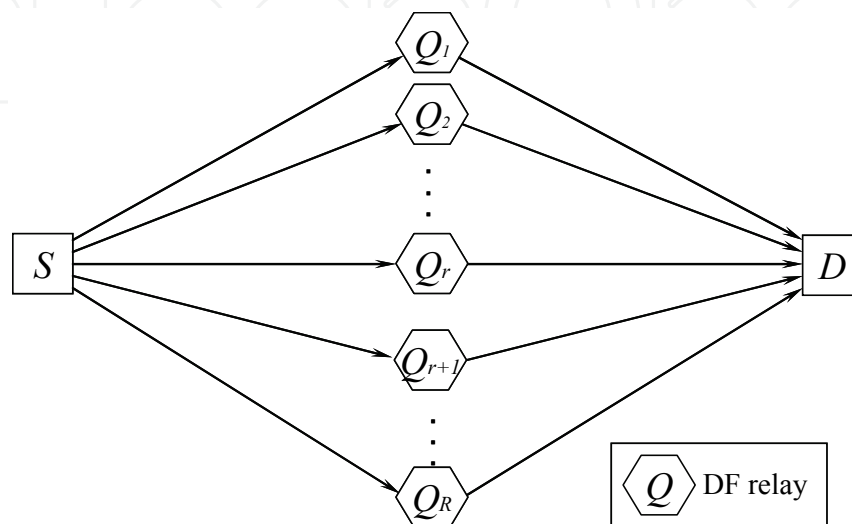


Fig. 11. Cooperative ZP-OFDM system architecture, (S : Source, D : Destination, Q_r : r -th Relay).

The matrix

$$\mathbf{T}_{ZP} = \begin{bmatrix} \mathbf{I}_N \\ 0 \end{bmatrix}_{P \times N} \quad (28)$$

performs the zero-padding on the transmitted signal with V zeros, where \mathbf{I}_N is $N \times N$ identity matrix, and $P = N + V$.

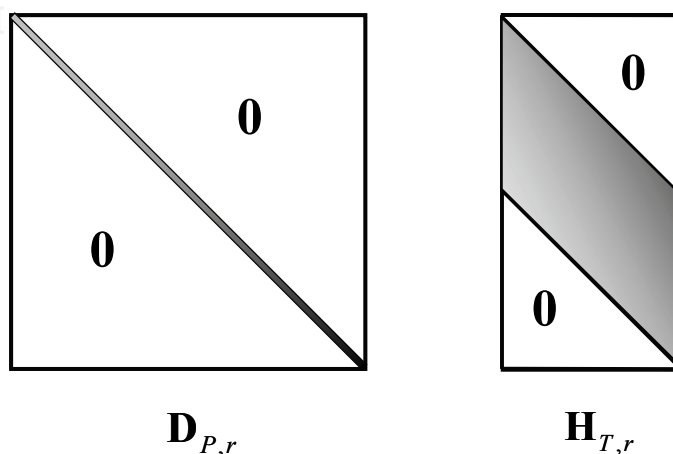


Fig. 12. Structure of (left) $\mathbf{D}_{P,r}$ and (right) $\mathbf{H}_{T,r}$ matrix. Blank parts are all 0's.

The matrix \mathbf{H}_r is a $P \times P$ lower triangular matrix with its first column vector is $[h_{1,r}, \dots, h_{L,r}, 0 \dots 0]^T$, and its first row vector is $[h_{1,r}, 0 \dots 0]$, and this matrix denotes the multipath channel over the r -th relay and destination link, L is the length of channel. Without loss of generality, we assumed that the channel lengths of different relay-destination links are all L . To avoid ISI, we should have $L \leq V$, and we assume $L = V$. The $\mathbf{D}_{P,r}$ is a diagonal matrix representing the residual carrier frequency error over the r -th relay and destination link and is defined in terms of its diagonal elements as $\mathbf{D}_{P,r} = \text{diag}(1, \alpha_r, \dots, \alpha_r^{P-1})$, with $\alpha_r = \exp(j2\pi\Delta q_r / N)$, $\text{diag}(\cdot)$ is diagonal matrix with main diagonal (\cdot) , and Δq_r is the normalized carrier frequency offset of r -th relay with the symbol duration of ZP-OFDM. Here, we notice that $\mathbf{H}_{T,r} = \mathbf{H}_r \mathbf{T}_{ZP}$ is a full column rank tall Toeplitz matrix, and its correlation matrix always guaranteed to be invertible. The structures of $\mathbf{D}_{P,r}$ and $\mathbf{H}_{T,r}$ can be shown as Fig. 12.

Since $\mathbf{H}_{T,r}$ relates to the linear convolution, we refer to this tall Toeplitz structure as linear structure, which assures symbol recovery (perfect detectability in the absence of noise) regardless of the channel zeros locations. The linear structure of ZP-OFDM provides a better BER performance and an easier blind channel estimation and blind symbol synchronization as well, while this is not the case for the CP-OFDM. In fact, the channel-irrespective symbol detectable property of ZP-OFDM is equivalent to claiming that ZP-OFDM enjoys maximum diversity gain. Intuitively, this can be understood as the ZP-OFDM retains the entire linear convolution of each transmitted symbol with the channel. Then, we will show how to use the linear property of $\mathbf{H}_{T,r}$ to achieve full spatial diversity in the cooperative system. Consequently, (27) can be rewritten as

$$\mathbf{y}_r = \mathbf{F}_{P,r} \mathbf{D}_{P,r} \mathbf{H}_{T,r} \mathbf{F}_{N,r}^H \mathbf{x}_r + \mathbf{n} \quad (29)$$

In this section, we consider a simple frequency division space frequency system for each relay \mathbf{x}_r , i.e., arranging transmitted symbols in different frequency bands according to the corresponding relay, as shown in the Fig. 13. By doing so, we can exploit the linear structure of ZP-OFDM to achieve the full cooperative diversity with linear receiver regardless of the existence of CFOs.

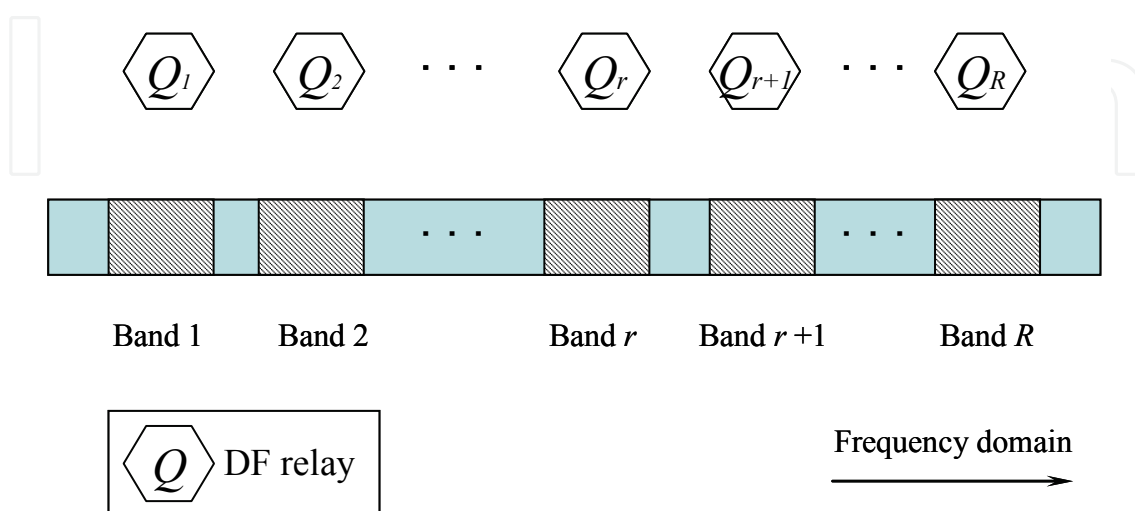


Fig. 13. Frequency division cooperative ZP-OFDM system.

We take \mathbf{x}_r as the information symbols correctly received at the r -th relay nodes involved in the DF-cooperative scheme. After full decoding, \mathbf{x}_r is assigned to the corresponding r -th frequency band as shown in the Fig. 13, and forwarded to the destination.

Considering the frequency division system, the received signal at the destination of all R relay nodes yields

$$\mathbf{y} = \mathbf{F}_p \mathbf{D} \mathbf{H} \mathbf{F}_N^H \mathbf{x} + \mathbf{n} \quad (30)$$

where $\mathbf{F}_p = \text{diag}(\mathbf{F}_{p,1}, \mathbf{F}_{p,2}, \dots, \mathbf{F}_{p,R})$, $\mathbf{D} = \text{diag}(\mathbf{D}_{p,1}, \mathbf{D}_{p,2}, \dots, \mathbf{D}_{p,R})$, $\mathbf{H} = \text{diag}(\mathbf{H}_{T,1}, \mathbf{H}_{T,2}, \dots, \mathbf{H}_{T,R})$, $\mathbf{F}_N^H = \text{diag}(\mathbf{F}_{N,1}^H, \mathbf{F}_{N,2}^H, \dots, \mathbf{F}_{N,R}^H)$ are all diagonal matrices with each relay's components on their diagonals. For instance, we consider a 2-relay cooperation system, i.e., $R = 2$, the structures of \mathbf{F}_p , \mathbf{D} , \mathbf{H} and \mathbf{F}_N^H can be illustrated as Fig. 14. In (30), $\mathbf{x} = [\mathbf{x}_1^T, \mathbf{x}_2^T, \dots, \mathbf{x}_R^T]^T$ denotes the forwarded signal from all relays occupying different frequency bands.

If we denote $\mathbb{H} = \mathbf{F}_p \mathbf{D} \mathbf{H} \mathbf{F}_N^H$, then (30) becomes

$$\mathbf{y} = \mathbb{H} \mathbf{x} + \mathbf{n} \quad (31)$$

On the other hand, let us go back to (27), right multiplying \mathbf{T}_{ZP} changes \mathbf{H}_r from a $P \times P$ lower triangular matrix into a $P \times N$ tall Toeplitz matrix $\mathbf{H}_{T,r}$ with its first column vector as $[h_{1,r}, \dots, h_{L,r}, 0 \dots 0]^T$, and we denote $\mathbf{x}_{t,r} = \mathbf{F}_{N,r}^H \mathbf{x}_r$, which is well known as time domain signal in OFDM system, then (27) can be represented as

$$\mathbf{y}_r = \mathbf{F}_{p,r} \mathbf{D}_{p,r} \mathbf{H}_{T,r} \mathbf{x}_{t,r} + \mathbf{n} \quad (32)$$

where $\mathbf{H}_{T,r} \mathbf{x}_{t,r}$ stands for the linear convolution of the multipath channel with the time domain transmitted signal, this is a special property possessed by the ZP-OFDM system. According to the commutativity of the linear convolution, we have $\mathbf{H}_{T,r} \mathbf{x}_{t,r} = \mathbf{X}_{T,r} \mathbf{h}_r$, where $\mathbf{X}_{T,r}$ is a $P \times L$ tall Toeplitz matrix with $[\mathbf{x}_{t,r}^T, \mathbf{0}^T]^T$ as its first column, and $\mathbf{h}_r = [h_{1,r}, \dots, h_{L,r}]^T$. Consequently, (32) can be transformed into another form as

$$\mathbf{y}_r = \mathbf{F}_{p,r} \mathbf{D}_{p,r} \mathbf{X}_{T,r} \mathbf{h}_r + \mathbf{n} \quad (33)$$

We denote $\mathbf{h}_c = [\mathbf{h}_1^T, \mathbf{h}_2^T, \dots, \mathbf{h}_R^T]^T$, $\mathbf{S}_r = \mathbf{F}_{p,r} \mathbf{D}_{p,r} \mathbf{X}_{T,r}$, $\mathbb{S} = \text{diag}(\mathbf{S}_1, \mathbf{S}_2, \dots, \mathbf{S}_R)$, and consider the received signal of all R relay nodes, then we get the received signal as

$$\mathbf{y} = \mathbb{S} \mathbf{h}_c + \mathbf{n} \quad (34)$$

Equations (31) and (34) are two equivalent received data models of this frequency division cooperative ZP-OFDM system. \mathbb{H} in (31) is regarded as the overall equivalent channel, while \mathbb{S} in (34) is the equivalent signal matrix of this frequency division cooperative ZP-OFDM system. In the following section, we will exploit \mathbb{H} and \mathbf{h}_c from (31) and (34) to show the verification of the full cooperative spatial diversity.

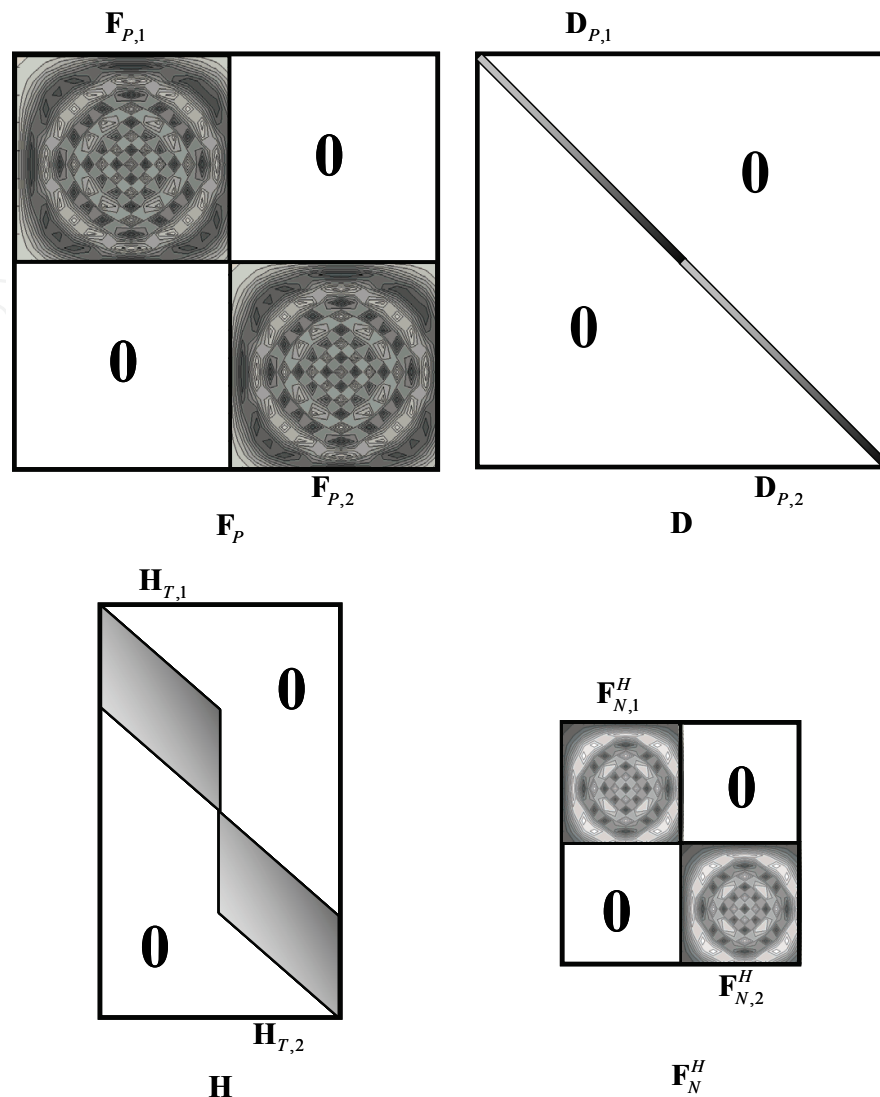


Fig. 14. Structures of the FFT matrices, CFOs matrix and channel matrix for 2-relay cooperative system, top left: FFT matrix \mathbf{F}_P , top right: CFOs matrix \mathbf{D} , bottom left: channel matrix: \mathbf{H} , bottom right: FFT matrix \mathbf{F}_N^H . Blank parts are all 0's.

4.3 Space time frequency coding design

4.3.1 Conditions of the full diversity with linear equalizer

In this section, we will show how linear receiver is the only required to achieve full cooperative diversity order RL . We first cite the following theorem from (Shang & Xia, 2007; Shang & Xia, 2008):

Theorem 2 (Shang & Xia, 2007; Shang & Xia, 2008): For PAM, PSK and square QAM constellations, if the following condition holds

$$\|\mathbf{H}\| \leq \alpha \|\mathbf{h}_c\| \quad \text{and} \quad \det(\mathbf{H}^H \mathbf{H}) \geq \beta \|\mathbf{h}_c\|^{2N}$$

where α and β are positive constants independent of \mathbf{h}_c , $\|\cdot\|$ is the Frobenius norm of a vector/matrix, and N is the number of symbols in the transmitted signal, i.e., the length of

\mathbf{x}_r in (29). Then, for any realization of \mathbb{H} , with ZF or MMSE receiver, full diversity can be achieved, i.e., the symbol error probability (SEP) P_e satisfies:

$$P_e(\hat{s}_l \rightarrow s_l) \leq \bar{c} \cdot \rho^{-RL}, \quad l=1,2,\dots,L$$

where $\bar{c} \triangleq \frac{\eta-1}{\eta} (a\hat{c})^{-2}$, η is the cardinality of the constellation, and $a = \frac{3}{2(\eta^2-1)}$,

$\frac{\sin^2(\pi/\eta)}{2}$ and $\frac{3}{4(\eta-1)}$ for PAM, PSK, and square QAM, respectively. $\hat{c} = \beta \left(\frac{L-1}{\alpha^2} \right)^{L-1}$,

and ρ is the symbol SNR.

In what follows, we will show that, with the STFC, the frequency division cooperative ZP-OFDM system satisfies the conditions in Theorem 2. In other words, the proposed frequency division system can achieve full diversity with linear receivers. Note that here the full diversity order is RL .

4.3.2 Space time frequency coding design and verification

According to the above mentioned conditions, we design a linear structure STFC, which guarantees the full cooperative spatial diversity and without redundant power gains. By right multiplying a matrix on $\bar{\mathbf{F}}_N^H \bar{\mathbf{x}}$, where \mathbf{I}_r is an $N \times N$ identity matrix, $r \in [1, 2, \dots, R]$,

$\bar{\mathbf{F}}_N^H = \mathbf{F}_{N,r}^H$ is an N -point IFFT matrix, and $\bar{\mathbf{x}} = \mathbf{x}_r \triangleq [x_0, \dots, x_{N-1}]^T$ stands for the frequency transmitted information signal, the received signal at the destination from all R relay nodes yields

$$\mathbf{y} = \mathbf{F}_p \mathbf{D} \mathbf{H} \mathbf{G} \bar{\mathbf{F}}_N^H \bar{\mathbf{x}} + \mathbf{n} \quad (35)$$

where \mathbf{F}_p , \mathbf{D} and \mathbf{H} are the same as (30). We denote $\mathbf{H} \mathbf{G} = \hat{\mathbf{H}}_T$ and $\bar{\mathbf{x}}_t = \bar{\mathbf{F}}_N^H \bar{\mathbf{x}}$, where $\hat{\mathbf{H}}_T = [\mathbf{H}_{T,1}^T, \mathbf{H}_{T,2}^T, \dots, \mathbf{H}_{T,R}^T]^T$, $\bar{\mathbf{x}}_t$ is the time domain signal. We notice that matrix \mathbf{G} spreads $\bar{\mathbf{x}}_t$ according to the corresponding relays, and forms a frequency division system, since the relays perform the forwarding in the different bands, as shown clearly in the Fig.13. Therefore, the Matrix \mathbf{G} can be regarded as a coding scheme on the time domain signal, for different relays and different bands, and so called space time frequency code. Then, (35) becomes

$$\mathbf{y} = \mathbf{F}_p \mathbf{D} \hat{\mathbf{H}}_T \bar{\mathbf{F}}_N^H \bar{\mathbf{x}} + \mathbf{n} \quad (36)$$

If we denote $\mathbb{H} = \mathbf{F}_p \mathbf{D} \hat{\mathbf{H}}_T \bar{\mathbf{F}}_N^H$ as the equivalent channel matrix, we get

$$\mathbf{y} = \mathbb{H} \bar{\mathbf{x}} + \mathbf{n} \quad (37)$$

We notice that $\hat{\mathbf{H}}_T$ is a linear Toeplitz matrix. Similar to (32) and (33), we have $\hat{\mathbf{H}}_T \bar{\mathbf{x}}_t = \hat{\mathbf{X}}_T \hat{\mathbf{h}}$, where $\hat{\mathbf{X}}_T$ is a $[P \times R] \times [P \times (R-1) + L]$ tall Toeplitz matrix with $[\bar{\mathbf{x}}_t^T, \mathbf{0}^T]^T$ as its first

column, and $\hat{\mathbf{h}} = [h_{1,1}, \dots, h_{L,1}, \mathbf{0}, h_{1,2}, \dots, h_{L,2}, \mathbf{0}, \dots, h_{1,R}, \dots, h_{L,R}]^T$ with length $[P \times (R-1) + L]$, Consequently, the equivalent STFC signal matrix could be formulated as

$$\mathbf{y} = \mathbb{S} \hat{\mathbf{h}} + \mathbf{n} \quad (38)$$

where $\mathbb{S} = \mathbf{F}_p \mathbf{D} \hat{\mathbf{X}}_T$.

Its proof is shown as follows. For the first condition, we have

$$\|\mathbb{H}\| \leq \|\mathbf{F}_p\| \|\mathbf{D}\| \|\hat{\mathbf{H}}_T\| \|\bar{\mathbf{F}}_N^H\| = \|\mathbf{F}_p\| \|\mathbf{D}\| \sqrt{N} \|\hat{\mathbf{h}}\| \|\bar{\mathbf{F}}_N^H\|$$

If we take $\alpha = \sqrt{N} \|\mathbf{F}_p\| \|\mathbf{D}\| \|\bar{\mathbf{F}}_N^H\|$, we have $\|\mathbb{H}\| \leq \alpha \|\hat{\mathbf{h}}\|$, and the first condition holds.

For the second condition, to continue the proof, we cite the results from (Zhang et al., 2005) in the following theorem:

Theorem 3 (Zhang et al., 2005): For any given positive integers p and q , there exists a positive constant c , such that for any nonzero vector \mathbf{v} , $\det(\mathcal{T}^H(\mathbf{v}, p, q) \mathcal{T}(\mathbf{v}, p, q)) \geq c \|\mathbf{v}\|^{2q}$ holds.

Here, we denote $\mathcal{T}(\mathbf{v}, p, q)$ as a Toeplitz matrix of size $(p+q-1) \times q$ as follows:

$$\mathcal{T}(\mathbf{v}, p, q) \triangleq \begin{bmatrix} v_1 & 0 & \cdots & 0 \\ v_2 & v_1 & \cdots & 0 \\ \vdots & \vdots & \ddots & \vdots \\ v_p & v_{p-1} & \cdots & 0 \\ 0 & v_p & \cdots & v_1 \\ \vdots & 0 & \cdots & v_2 \\ \vdots & \vdots & \ddots & \vdots \\ 0 & 0 & 0 & v_p \end{bmatrix}$$

where $\mathbf{v} = [v_1, v_2, \dots, v_p]^T$ is any non-zeros column vector of length p .

Consequently, note that \mathbf{F}_p , \mathbf{D}_p and $\bar{\mathbf{F}}_N^H$ are all unitary matrices, we have

$$\begin{aligned} \det(\mathbb{H}^H \mathbb{H}) &= \det(\bar{\mathbf{F}}_N) \det(\bar{\mathbf{F}}_N^H) \det(\hat{\mathbf{H}}_T^H \hat{\mathbf{H}}_T) \\ &= \det(\hat{\mathbf{H}}_T^H \hat{\mathbf{H}}_T) \end{aligned}$$

where $\det(\bar{\mathbf{F}}_N) \det(\bar{\mathbf{F}}_N^H) = 1$, and $\hat{\mathbf{H}}_T$ is a tall Toeplitz matrix. According to the Theorem 3, it is easy to show

$$\det(\mathbb{H}^H \mathbb{H}) = \det(\hat{\mathbf{H}}_T^H \hat{\mathbf{H}}_T) \geq \beta \|\hat{\mathbf{h}}\|^{2N}$$

where β is a positive constant as shown in Theorem 2, and the second condition of theorem 2 holds. Therefore, the proposed STFC can achieve the full diversity for the cooperative ZP-OFDM system with CFOs and multipath channel.

According to the above full diversity scheme, we notice that the tall Toeplitz structure of the ZP-OFDM channel matrix is a unique advantage, which is not possessed by CP-OFDM. How to design a space time code or space frequency code to obtain the tall Toeplitz structure or linear convolutional structure is the key element to achieve full diversity in a cooperative wireless system.

4.4 Simulation results

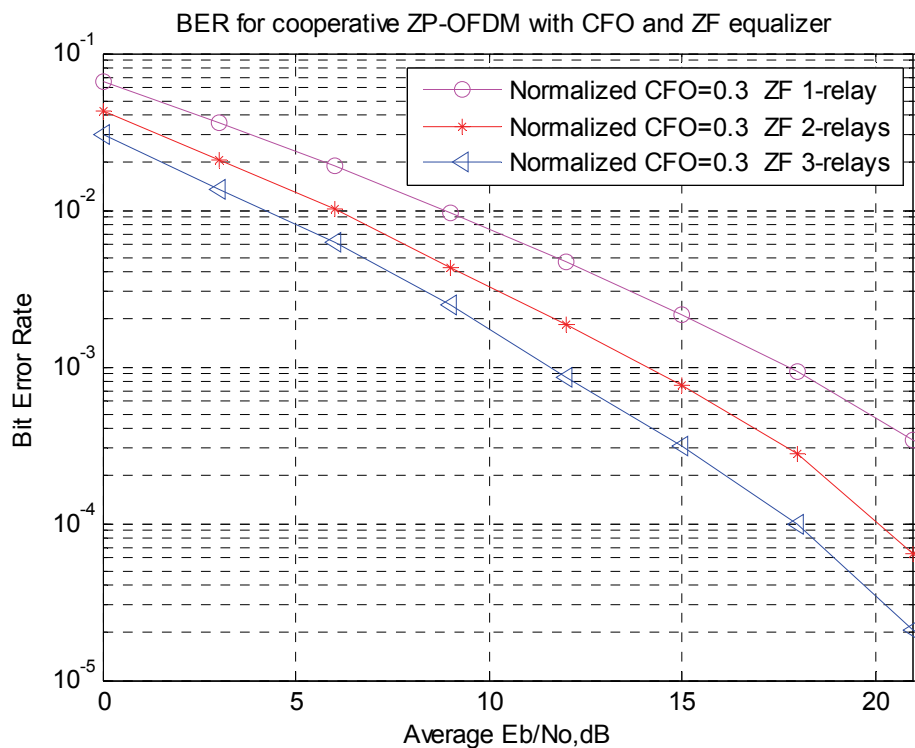


Fig. 15. BER performance of STFC cooperative ZP-OFDM with the same CFO and ZF equalizer.

Now, we present simulation results of the performance of our STFC design. For different numbers of relays with ZF equalizer, Fig. 15 shows the BER vs. E_b/N_0 performance under the same CFO, and $\Delta q_r = 0.3$. The diversity order can be shown as the asymptotic slope of BER vs. E_b/N_0 curve. It describes how fast the error probability decays with SNR. We can see from Fig. 15 that the full cooperative diversity is achieved with the ZF equalizer, because the asymptotic slope of the curve increases with the increasing of the number of relays.

Fig. 16 shows the BER vs. E_b/N_0 performance with different CFOs and with MMSE equalizer. We assume that the absolute value of CFOs is less than half of the subcarrier spacing, i.e., $\Delta q_r \in (-0.5, 0.5)$. It can be seen that, the E_b/N_0 gaps between $\Delta q_r = 0.01$ and $\Delta q_r = 0.5$ are very small. Although the increasing of CFOs will not change the diversity orders, it will deteriorate the BER performance because larger CFOs result in larger approximation error. In other words, larger CFOs will increase the power of equivalent noise and consequently degrade the communication performance. We can also see that the full cooperative diversity is achieved with the MMSE equalizers. Compared to ZF equalizer, the BER performance of MMSE equalizer is much better. In the Fig. 16, even with the severer CFOs, diversity increases with increasing the number of relays. From the figure, we also

notice that, without the proposed STFC, i.e., direct combining of the 2-relay signals at the destination, the 2-relays system only yields 3 dB power gain. The 2-relay BER vs. E_b/N_0 curve without STFC is parallel to the 1-relay case, indicating no diversity is achieved.

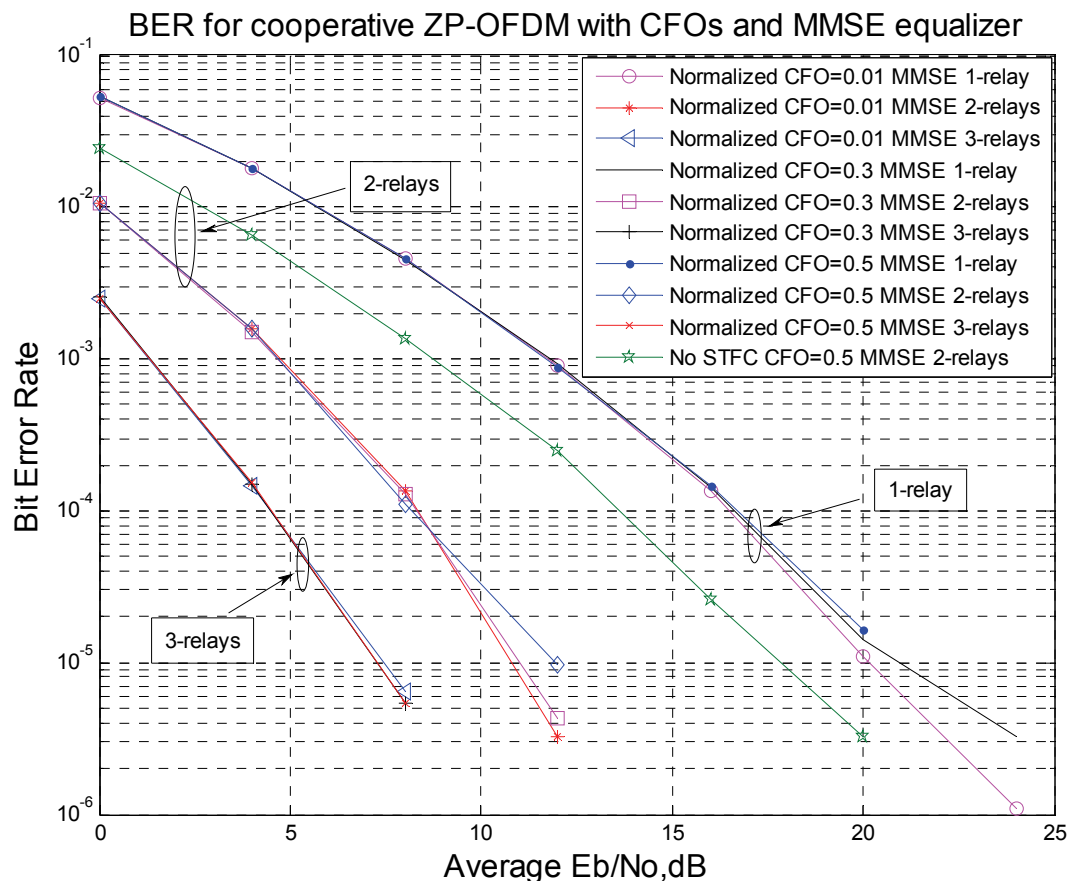


Fig. 16. BER performance of linear freq. div. STFC cooperative ZP-OFDM with the different CFOs and MMSE equalizer.

5. Conclusions

In this chapter, we investigated some cooperative OFDM communication issues, such as relay selection and full diversity design. First, we proposed a hybrid OFDM cooperative strategy for multi-node wireless networks employing both DF and AF relaying. Fully decoding is guaranteed by simply comparing SNRs at relay nodes to the SNR threshold, which is more efficient than utilizing conventional cyclic redundant checking code. The lower bound and the upper bound of the SNR threshold were provided as well. After correct decoding, the DF protocol outperforms AF protocol in terms of BER performance, which can be seen from the Monte Carlo simulation as well as analytical results. These results justify that the DF protocol dominates hybrid cooperation strategy. For the suggested hybrid DF-AF cooperation protocol, we also represented a dynamic optimal combination strategy for the optimal AF selection. The closed-form BER expression of the hybrid OFDM cooperation in Rayleigh fading channel was derived. The agreement between the analytical curves and numerical simulated results shows that the derived closed-form BER expression is suitable for the DF-dominant hybrid cooperation protocols. The compact

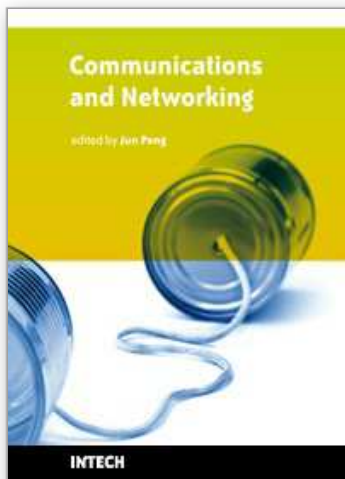
and closed-form BER expression can easily provide an insight into the results as well as a heuristic help for the design of future cooperative wireless systems. Subsequently, we investigated the cooperative ZP-OFDM communication with multiple CFOs and multipath channel, i.e., with ICI and ISI. In the ZP-OFDM system, the linear structure, or tall Toeplitz structure of channel matrix is a unique feature. Therefore, we provided a simple frequency division cooperative ZP-OFDM system to illustrate the full diversity design, and showed that some power expenditure was needed for the proposed frequency division cooperative ZP-OFDM system to achieve full cooperative diversity. Then, we proposed another power efficient STFC, taking advantage of the linear structure of ZP-OFDM, to achieve the full cooperative diversity. Furthermore, we also showed that, linear equalizations, such as ZF and MMSE equalizers, can be used to collect the full cooperative spatial diversity gain. Comparing to exhausted ML decoding methods, the computational complexity is greatly reduced.

6. References

- Lima, P.; Bonarini, A. & Mataric, M. (2004). *Name of Book in Italics*, Publisher, ISBN, Place of Publication
- Batra, A. Multi-band OFDM physical layer proposal for IEEE 802.15 Task Group 3a IEEE P802.15-04/0493r1, Sep. 2004.
- Batra, A.; Balakrishnan, J.; Aiello, G. R. & Dabak, A. (2004). Design of a multiband OFDM system for realistic UWB channel environments, *IEEE Transaction on Microwave and Techniques*, Vol. 52, No. 9, pp. 2123–2138, ISSN: 0018-9480
- Barbarossa, S. (2005). *Multiantenna Wireless Communication Systems*, MA: Artech House, ISBN-13: 978-1580536349, Norwood
- Cover, T. M. & El Gamal, A. A. (1979). Capacity theorems for the relay channel, *IEEE Trans. Inform. Theory*, Vol. 25, No. 5, pp. 572–584, ISSN: 0018-9448
- Farhadi, G. & Beaulieu, N. C. (2008). On the Ergodic Capacity of Wireless Relaying System over Rayleigh Fading Channels, *IEEE Trans. Wireless Communications*, Vol. 7, No. 11, pp. 4462–4467, ISSN: 1536-1276
- Foschini, G. J. & Gans, M. (1998). On the limits of wireless communication in a fading environment when using multiple antennas, *Wireless Personal Commun.*, Vol. 6, pp. 311–335, ISSN: 0929-6212
- Hasna, M. O. & Alouini, M. -S. (2002). Performance analysis of two-hop relayed transmissions over Rayleigh-fading channels, *Proceedings of Vehicular Technology Conf.* 2002, pp. 1992–1996, Birmingham, AL
- Hwang, J.; Consulto, R. R. & Yoon, H. (2007) 4G mobile networks - technology beyond 2.5G and 3G. In *PTC*, 2007.
- Kramer, G.; Gastpar, M. & Gupta, P. (2005). Cooperative strategies and capacity theorems for relay networks, *IEEE Trans. Inf. Theory*, Vol. 51, pp. 3037–3063, ISSN: 0018-9448
- Laneman, J. N.; Tse, D. N. C. & Wornell, G. W. (2004). Cooperative diversity in wireless networks: efficient protocols and outage behavior. *IEEE Trans. Inform. Theory*, Vol. 50, No. 12, pp. 3062–3080, ISSN: 0018-9448
- Li, Y.; Zhang, W. & Xia, X. (2009). Distributive high rate space-frequency codes achieving full cooperative and multipath diversities for asynchronous cooperative communications, *IEEE Trans. Vehicular Technology*, Vol. 58, No. 1, pp. 207–217, ISSN: 0018-9545

- Lin, S. & Costello, D. J. Jr. (1983). *Error Control Coding: Fundamentals and Applications.*, NJ: Prentice-Hall, ISBN: 013283796X, Englewood Cliffs
- Liu, Z.; Xin, Y. & Giannakis, G. B. (2003). Linear constellation precoded OFDM with maximum multipath diversity and coding gains, *IEEE Trans. Commun.*, Vol. 51, No. 3, pp. 416–427, ISSN: 0090-6778
- Liu, K. J. R.; Sadek, A. K.; Su W. & Kwasinski, A. (2009). *Cooperative communications and networks*, Cambridge University Press, ISBN-13 978-0-521-89513-2, Cambridge
- Louie, R.; Li, Y.; Suraweera, H. A. & Vucetic, B. (2009). Performance analysis of beamforming in two hop amplify and forward relay network with antenna correlation, *IEEE Trans. Wireless Communications*, Vol. 8, No. 6, pp. 3132–3141, ISSN: 1536-1276
- Lu, H.; Nikoosar, H. & Lian, X. (2010). Performance evaluation of hybrid DF-AF OFDM cooperation in Rayleigh Channel, to appear in European Wireless Technology Conference, 2010
- Lu, H. & Nikoosar, H. (2009). A thresholding strategy for DF-AF hybrid cooperative wireless networks and its performance, *Proceedings of IEEE SCVT '09*, UCL, Louvain. Nov. 2009
- Lu, H.; Nikoosar, H. & Chen, H. (2009). On the potential of ZP-OFDM for cognitive radio, *Proceedings of WPMC'09*, pp. 7-10, Sendai, Japan. Sep. 2009
- Ma, X. & Zhang, W. (2008). Fundamental limits of linear equalizers: diversity, capacity, and complexity, *IEEE Trans. Inform. Theory*, Vol. 54, No. 8, pp. 3442–3456, ISSN: 0018-9448
- Muquet, B.; Wang, Z.; Giannakis, G. B.; Courville, M. & Duhamel, P. (2002). Cyclic prefixing or zero padding for wireless multicarrier transmissions, *IEEE Transaction on Communications*, Vol. 50, No. 12, pp. 2136–2148, ISSN: 0090-6778
- Nosratinia, A.; Hunter, T. E. & Hedayat, A. (2004). Cooperative communication in wireless networks, *IEEE Commun. Mag.*, Vol. 42, pp. 74–80, ISSN: 0163-6804
- Patel, C.; Stüber, G. & Pratt, T. (2006). Statistical properties of amplify and forward relay fading channels, *IEEE Trans. Veh. Technol.*, Vol. 55, No. 1, pp. 1-9, ISSN: 0018-9545
- Proakis, J. G. (2001). *Digital Communications*, 4th ed., McGraw Hill, ISBN-13: 978-0072321111, New York
- Sadek, A. K.; Su, W. & Liu, K. J. R. (2007). Multi-node cooperative communications in wireless networks, *IEEE Trans. Signal Processing*, Vol. 55, No. 1, pp. 341–355, ISSN: 1053-587X
- Sendonaris, A.; Erkip, E. & Aazhang, B. (2003). User cooperation diversity – Part I: System description, *IEEE Trans. Commun.*, Vol. 51, No. 11, pp. 1927–1938, ISSN: 0090-6778
- Sendonaris, A.; Erkip, E. & Aazhang, B. (2003). User cooperation diversity – Part II: Implementation aspects and performance analysis, *IEEE Trans. Commun.*, Vol. 51, No. 11, pp. 1939–1948, ISSN: 0090-6778
- Shang, Y. & Xia, X.-G. (2007). A criterion and design for space-time block codes achieving full diversity with linear receivers, *Proceedings of IEEE ISIT'07*, Nice, France, pp. 2906–2910, June 2007
- Shang, Y. & Xia, X.-G. (2008). On space-time block codes achieving full diversity with linear receivers, *IEEE Trans. Inform. Theory*, Vol. 54, pp. 4528–4547, ISSN: 0018-9448
- Standard ECMA-368 High Rate Ultra Wideband PHY and MAC Standard, 3rd edition, Dec. 2008

- Tse, D. N. C. & Viswanath, P. (2005). *Fundamentals of Wireless Communications.*, U.K.: Cambridge Univ. Press, ISBN-13: 9780521845274, Cambridge
- Wang, Z. & Giannakis, G. B. (2000). Wireless multicarrier communications: Where Fourier meets Shannon, *IEEE Signal Processing Mag.*, Vol. 17, No. 3, pp. 1-17, ISSN: 1053-5888
- Zhang, J.-K.; Liu, J. & Wong, K. M. (2005). Linear Toeplitz space time block codes, Proceedings of IEEE ISIT'05, Adelaide, Australia, Sept. 2005



Communications and Networking

Edited by Jun Peng

ISBN 978-953-307-114-5

Hard cover, 434 pages

Publisher Sciyo

Published online 28, September, 2010

Published in print edition September, 2010

This book "Communications and Networking" focuses on the issues at the lowest two layers of communications and networking and provides recent research results on some of these issues. In particular, it first introduces recent research results on many important issues at the physical layer and data link layer of communications and networking and then briefly shows some results on some other important topics such as security and the application of wireless networks. In summary, this book covers a wide range of interesting topics of communications and networking. The introductions, data, and references in this book will help the readers know more about this topic and help them explore this exciting and fast-evolving field.

How to reference

In order to correctly reference this scholarly work, feel free to copy and paste the following:

Hao Lu, Homayoun Nikookar and Tao Xu (2010). OFDM Communication with Cooperative Relays, Communications and Networking, Jun Peng (Ed.), ISBN: 978-953-307-114-5, InTech, Available from: <http://www.intechopen.com/books/communications-and-networking/ofdm-communication-with-cooperative-relays>

INTECH
open science | open minds

InTech Europe

University Campus STeP Ri
Slavka Krautzeka 83/A
51000 Rijeka, Croatia
Phone: +385 (51) 770 447
Fax: +385 (51) 686 166
www.intechopen.com

InTech China

Unit 405, Office Block, Hotel Equatorial Shanghai
No.65, Yan An Road (West), Shanghai, 200040, China
中国上海市延安西路65号上海国际贵都大饭店办公楼405单元
Phone: +86-21-62489820
Fax: +86-21-62489821

© 2010 The Author(s). Licensee IntechOpen. This chapter is distributed under the terms of the [Creative Commons Attribution-NonCommercial-ShareAlike-3.0 License](https://creativecommons.org/licenses/by-nc-sa/3.0/), which permits use, distribution and reproduction for non-commercial purposes, provided the original is properly cited and derivative works building on this content are distributed under the same license.

IntechOpen

IntechOpen